

# Alongshore Variability in Coastal Dune Erosion and Post-Storm Recovery, Northern Coast of France

Arnaud Héquette<sup>†</sup>, Marie-Hélène Ruz<sup>†</sup>, Amar Zemmour<sup>†</sup>, Denis Marin<sup>†</sup>, Adrien Cartier<sup>§</sup>, and Vincent Sipka<sup>†</sup>

<sup>†</sup>UMR 8187 LOG  
Univ. Littoral Cote d'Opale  
Laboratoire d'Océanologie et de Géosciences  
Wimereux, France

<sup>§</sup>GEODUNES  
Rosendaël, France



www.cerf-jcr.org



www.JCRonline.org

## ABSTRACT

Héquette, A.; Ruz, M.H.; Zemmour, A.; Marin, D.; Cartier, A., and Sipka, V., 2019. Alongshore Variability in Coastal Dune Erosion and Post-Storm Recovery, Northern Coast of France. In: Castelle, B. and Chaumillon, E. (eds.), *Coastal Evolution under Climate Change along the Tropical Overseas and Temperate Metropolitan France. Journal of Coastal Research*, Special Issue No. 88, pp. 25–45. Coconut Creek (Florida), ISSN 0749-0208.

As along many parts of the world's shoreline, the coastal dunes extending along the macrotidal coast of northern France represent important defenses against marine flooding. The impacts of storms on the upper beach and foredunes and their post-storm recovery were analyzed using nearly 10 years of offshore wave measurements, water level records, wind measurements, and in situ and airborne LiDAR topographic surveys of the beach and foredunes. Our results show that coastal dunes located at a relatively short distance apart along a coastal stretch with the same wave exposure can have significantly different responses to storms. Not only the impacts of storm events were greater on some dunes, but post-storm recovery also varied from one foredune to another. A strong alongshore variability in dune erosion and recovery was observed with a positive eastward gradient in dune volume change, probably related to longshore and onshore-directed sediment supply. Our measurements revealed that even where the foredune underwent significant erosion during the first years of the survey period, progressive full dune recovery took place through the development of a sand ramp at the dune toe that favored landward sediment transport from the upper beach to the foredune. This period was followed by an unusual series of closely spaced storms during fall-winter 2013-2014 that had major impacts on the coasts of Western Europe. Several of these storms were responsible for extreme water levels, which resulted in significant retreat of the dune front and massive volume loss in places. Our analyses show that the maximum water levels reached during storms represent a major factor explaining dune erosion compared to wave energy that is of secondary importance along this macrotidal coast. Our results also suggest that dune volume change during storms and subsequent recovery were largely controlled by the initial dune and upper beach morphology. A strong correspondence was found between dune front volume change and initial upper beach width and with dune toe elevation, but a somewhat weaker relationship was observed between dune volume change and initial dune height.

**ADDITIONAL INDEX WORDS:** *Foredune, storm erosion, post-storm dune recovery, North Sea.*

## INTRODUCTION

The coastal dunes of northern France, as along many parts of the world's coastlines, represent important defenses against marine flooding since large areas of the coastal zone of the region consist of low reclaimed lands located below mean high water level (Maspataud, Ruz, and Vanhée, 2012; Rufin-Soler, Héquette, and Gardel, 2008). Because dune erosion and marine flooding will likely increase in the next future with rising sea level associated with climate change (Neumann *et al.*, 2015; Nicholls and Cazenave, 2010), the morphological behavior and evolution of the coastal dunes of northern France, notably in response to storm events and climatic variability, has received a growing attention during the last few years (Crapoulet *et al.*, 2017; Idier *et al.*, 2013; Ruz, Héquette, and Maspataud, 2009). Despite these

recent efforts, there is still a gap in our understanding of the morphodynamic behavior of the coastal dunes of the region, particularly concerning their response to storms and subsequent post-storm recovery mechanisms that were scarcely investigated along this macrotidal coast (Maspataud, Ruz, and Héquette, 2009).

In addition to being natural barriers protecting low-lying coastal areas from marine flooding and storm wave erosion (Pye *et al.*, 2007; Spalding *et al.*, 2014), coastal dunes also represent valuable assets for recreation and tourism, and for nature conservation as they are unique ecosystems that house protected and endangered species (Pinna *et al.*, 2015; Van der Beist *et al.*, 2017). Shoreline retreat and long-term dune erosion result in a decrease in the ecosystem services provided by coastal dunes that can support the maintenance of coastlines and may contribute to adaptation to future sea level rise (Hanley *et al.*, 2014; Spalding *et al.*, 2014). Therefore, there is a need for a better understanding of coastal dune dynamics, and notably of their responses to storms and rebuilding phases during post-storm recovery, to increase our

DOI: 10.2112/SI88-004.1 received 6 July 2018; accepted in revision 7 December 2018.

\*Corresponding author: arnaud.hequette@univ-littoral.fr

©Coastal Education and Research Foundation, Inc. 2019

ability to predict their future evolution, which may be particularly valuable to coastal managers.

Coastal dunes are highly dynamic environments closely linked to the adjacent beach through complex interactions over a wide range of temporal and spatial scales (Castelle *et al.*, 2017; Hesp, 1988; Houser, Hapke, and Hamilton, 2008; Houser and Ellis, 2013; Psuty, 1988; Puijenbroek *et al.*, 2017; Short and Hesp, 1982; Walker *et al.*, 2017). The impacts of storms on coastal dunes have been extensively studied (*e.g.*, Burvingt *et al.*, 2018; Castelle *et al.*, 2015; Cooper *et al.*, 2004; Dissanayake *et al.*, 2015; Esteves *et al.*, 2012; Karunarathna *et al.*, 2014; Masselink *et al.*, 2016; Ruz, Héquette, and Maspataud, 2009) which provided significant insights into the different processes and mechanisms responsible for dune erosion. Overall, these studies showed that the response of coastal dunes to storms is highly variable and is not only a function of wave energy, storm duration and maximum surge height reached during the event, but that it also depends on the initial (pre-storm) dune and beach morphology, notably dune height (Hesp, 2002; Houser, Hapke, and Hamilton, 2008; Houser and Hamilton, 2009; Mathew, Davidson-Arnott, and Ollerhead, 2010), upper beach volume and width (Crapoulet *et al.*, 2017; Keijsers *et al.*, 2014; Pye and Blott, 2016a), shoreline orientation relative to incoming storm waves (Burvingt *et al.*, 2017; Cooper *et al.*, 2004; Le Mauff *et al.*, 2018; Pye and Blott, 2016b), size and position of intertidal or nearshore bars (Castelle *et al.*, 2015; Davidson-Arnott and Stewart, 1987; Scott *et al.*, 2016), and beach types, wide and gently sloping dissipative beaches providing more protection to the dune front during storms than steep reflective beaches (Hesp and Walker, 2013; Short and Hesp, 1982).

Compared to studies that documented dune erosion during storm events, post-storm dune recovery has received much less attention. In contrast to dune erosion that may occur within a few hours during a storm, the post-storm recovery of coastal dunes is a much slower process that generally takes several years and up to decades (Houser *et al.*, 2015; Morton, Paine, and Gibeaut, 1994). Nevertheless, there is a paucity of data on long-term beach recovery and except for a few studies based on long-term monitoring of beach and coastal dunes (Burvingt *et al.*, 2018; Houser *et al.*, 2015; Suanez *et al.*, 2015), most studies have been focused on the immediate to short-term recovery of coastal dunes following storms (*e.g.*, Castelle *et al.*, 2017; Houser and Hamilton, 2009; Katuna, 1991; Scott *et al.*, 2016). It is also noteworthy that the majority of observations of dune recovery were conducted in micro- to mesotidal settings and that observations of post-storm dune recovery processes are still extremely limited along macrotidal coasts (Maspataud, Ruz, and Héquette, 2009; Suanez *et al.*, 2012, 2015) where large fluctuations of water levels may potentially result in significant variations in dry beach width (Anthony, Ruz, and Vanhée, 2009; Ruz and Meur-Férec, 2004) which strongly controls the quantity of sediment that may be transported back to the dunes by aeolian processes.

Studies dedicated to dune erosion and recovery also revealed that the response of beach-dune systems to storms and subsequent recovery is usually not spatially uniform and that beach-dune profile changes often show considerable alongshore variability (Brooks, Spencer, and Christie, 2017; de Winter, Gongriep, and Ruessink, 2015; Houser, Hapke, and Hamilton, 2008; Kahn and

Roberts, 1982; Splinter *et al.*, 2018; Suanez *et al.*, 2012;). Several studies suggested that this variability may be due to alongshore variations in dune height (Houser, Hapke, and Hamilton, 2008, 2015; Houser, 2013), in beach slope (Larson, Erikson, and Hanson, 2004), in upper beach width (Crapoulet *et al.*, 2017; Pye and Blott, 2016a), in dune toe elevation (Splinter *et al.*, 2018), or in wave height and wave run-up elevation (Ruggiero *et al.*, 2001). Other possible causes of spatially variable responses of coastal dunes are localized rip currents (Loureiro, Ferreira, and Cooper, 2012), presence (or absence) of sand bars and of their morphological characteristics (Castelle *et al.*, 2015; Harley *et al.*, 2009), as well as offshore bathymetry through wave refraction over inner shelf sand ridges or sand banks (Héquette *et al.*, 2009; Houser, Hapke, and Hamilton, 2008; Houser and Hamilton, 2009) that can induce gradients in longshore sediment transport (Houser and Mathew, 2011), which in turn may be responsible for alongshore variability in the morphology of foredunes and in their storm response (Houser, 2013). Although the observations gathered through these studies contributed to improve our knowledge of the alongshore variations in the response of coastal dune to storms and to post-storm recovery processes, the exact mechanisms responsible for this variability remain poorly understood.

In this paper, we present results obtained on the evolution of coastal dunes located between Dunkirk and the Belgium border (Figure 1) based on several airborne LiDAR topographic surveys and on recurrent *in situ* topographic profile measurements over almost 10 years (2007 to 2016) at two nearby sites with contrasting morphological evolutions. These data were used in combination with wave, wind and water level measurements to assess the impacts of storm events on the upper beach and foredunes and analyze their post-storm evolution in order to get some insights into the factors explaining the differences in their morphological behavior (*i.e.*, accretion, stability or erosion). In particular we investigate the impact of the series of storms that struck the Western Europe coastlines during the autumn and winter 2013-2014 (Brooks, Spencer, and Christie, 2017; Castelle *et al.*, 2015; Pye and Blott, 2016a), which is one of the stormiest periods of the last decades (Masselink *et al.*, 2016; Matthews *et al.*, 2014). These results eventually lead to a discussion of the possible impacts of climate change on the coastal dunes of the region and more specifically on coastal dunes in macrotidal coastal environments.

## STUDY AREA

Despite a considerable expansion of urban and port areas during the 20<sup>th</sup> century, coastal dunes are still widely distributed along the coast of northern France that extends over 55 km between the Cap Blanc Nez chalk cliffs to the Belgium border (Figure 1). The coast essentially consists of wide and gently sloping sandy beaches with multiple intertidal bars (Anthony *et al.*, 2005; Reichmüth and Anthony, 2007) backed by coastal dunes that commonly exceed 10 m high and reach up to 25 m in places (Battiau-Queney *et al.*, 2001; Ruz, Anthony, and Faucon, 2005). The dunes merge with the low-lying reclaimed lands of the French part of the Flemish coastal plain that extends 10 to 20 km landward. Offshore, tidal sand banks are widespread across the nearshore zone and the inner shelf where they form extensive

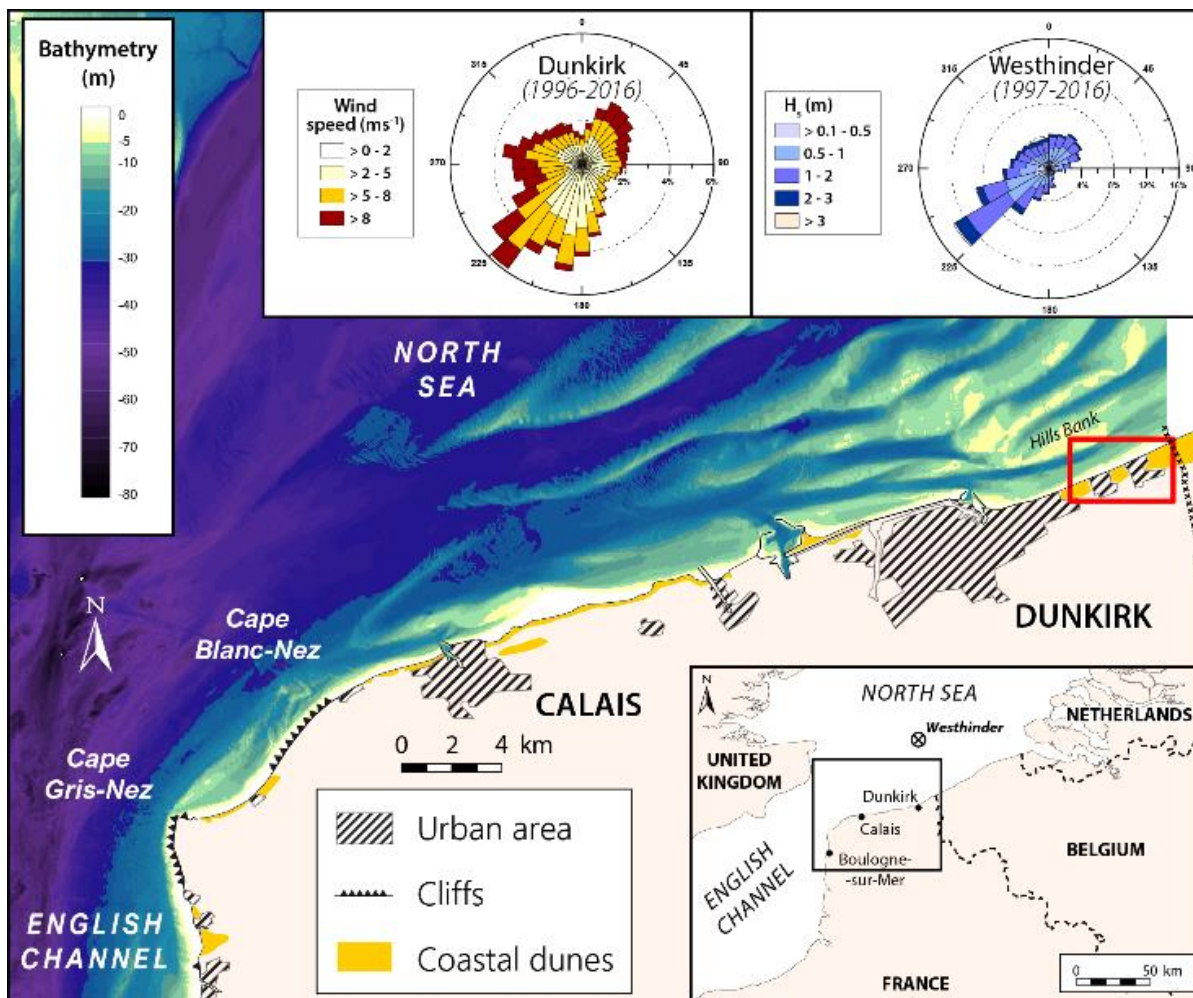


Figure 1. Location map of the study area. The rectangle on the right hand side of the main map corresponds to the location of the study site. Wind rose is based on hourly wind speeds and directions from Météo-France weather station in Dunkirk; wave rose is based on bi-hourly significant wave heights measured at the Westhinder offshore wave buoy (see inset for location). Bathymetry from 2015 French Hydrographic Survey (SHOM) data base.

linear sand bodies sub-parallel to the shoreline (Augris, Clabaut, and Vicaire, 1990; Beck *et al.*, 1991).

During the last fifteen years or so, a series of studies carried out on the recent evolution of northern France coastal dunes showed contrasting dynamics throughout the region (*e.g.*, Vasseur and Héquette, 2000; Chaverot *et al.*, 2008; Maspataud, Ruz, and Héquette, 2011; Ruz *et al.*, 2017). Although several papers pointed out that coastal dune erosion was common along the coast of northern France during the last decades (Aernouts and Héquette, 2006; Clabaut, Chamley, and Marteel, 2000; Ruz and Meur-Férec, 2004; Ruz, Héquette, and Maspataud, 2009), it was also shown that coastal dunes were stable in several areas, at least during discrete time periods (Battiau-Queney *et al.*, 2003; Ruz, Anthony, and Faucon, 2005). Coastal dune development that resulted in shoreline progradation was also observed in places (Chaverot *et al.*, 2008; Ruz, Héquette, and Marin, 2017; Ruz *et al.*,

*et al.*, 2017), particularly where the onshore migration of nearshore sand banks resulted in substantial sediment supply from the shoreface (Anthony, 2013; Héquette and Aernouts, 2010).

The extreme northern coastline of France has been massively transformed by urban and port development (Ruz, Anthony, and Faucon, 2005) and the only stretch of preserved dune barrier is located east of the port of Dunkirk (Figure 1). From Dunkirk to the Belgium border, inland parabolic dunes fronted by an established foredune form a 7 km long well-developed coastal dune system, 5 to 25 m high and 700 to 1400 m wide (Clabaut, Chamley, and Marteel, 2000). This coastal dune field is interrupted by the coastal resorts of Zuydcoote and Bray-Dunes and is divided in three coastal dune sectors: the *Dune Dewulf* to the west, the *Dune Marchand* and the *Dune du Perroquet* to the east (Figure 2A). Shoreline change analyses using series of aerial photographs revealed spatially contrasted evolution along this

coast since the middle of the 20<sup>th</sup> century (Maspataud, Ruz, and Héquette, 2011). Along the *Dune Marchand* in the central part of this coastal stretch, the shoreline experienced both erosion and progradation since the late 1950s, but was overall fairly stable (Figure 2B). Conversely, the shoreline retreated up to 50 m along the *Dune Dewulf* during the same time interval while progradation was observed along the *Dune du Perroquet*, resulting in a seaward shoreline displacement of about 40 m in places.

The present morphology of the dune front still reflects these evolutionary trends of the shoreline. To the west (*Dune Dewulf*), the established foredune is 50 m to 150 m wide and is mostly 6 to 10 m high (Figure 3A) with a steep stoss slope partly vegetated

(Figure 2C). The alongshore variation in dune height is partly due to the presence of beach access paths and dune trampling and to localized deflation corridors (Figure 2C, P1). The junction between the dune toe and the foreshore is a narrow (20-30 m wide) upper beach. To the east, the foredune height tends to decrease with a maximum dune height hardly exceeding 8 m along the *Dune Marchand* (Figure 3A).

Along the *Dune du Perroquet* the crest of the foredune is generally less than 6 m high, with a gentle well vegetated seaward slope (Figure 2C). In this area, incipient foredunes develop at the upper beach-dune toe during summer. The width of the foredune front strongly reflects the recent shoreline evolution, the foredune front being generally much narrower along the erosion-dominated

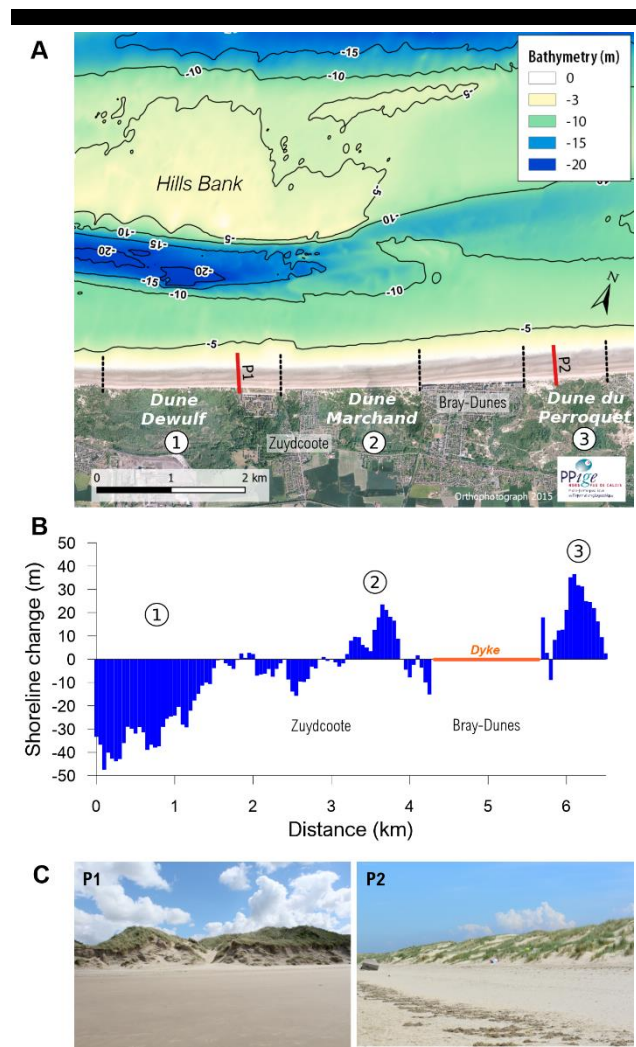


Figure 2. (A) Vertical aerial photograph showing the location of the different coastal dune sectors and of the topographic profiles P1 and P2, and nearshore bathymetry (depth soundings from 2015 French Hydrographic Survey (SHOM) data base); (B) Shoreline change from 1949 to 2015 between Dunkirk and the Belgium border based on orthophotos; (C) Ground photographs of the dune front in the vicinity of profile P1 (July 2016) and of profile P2 (June 2018).

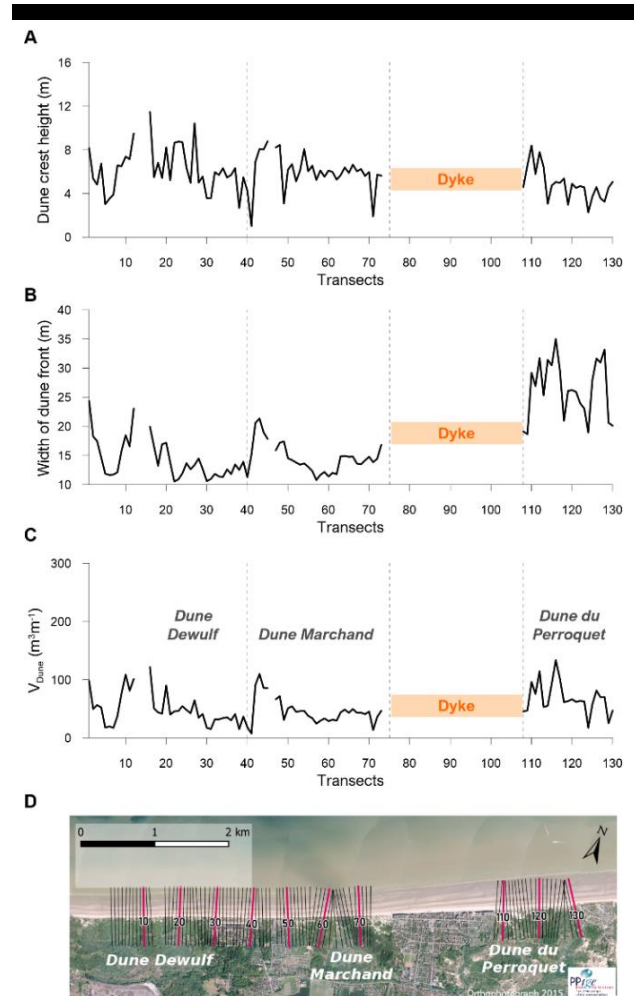


Figure 3. Longshore variations in (A) dune crest height, (B) width of dune front, and (C) coastal dune volume ( $V_{Dune}$ ) between Dunkirk and the Belgium border based on airborne LiDAR topographic data collected in May 2016 (measurements were carried out along cross-shore transects spaced 50 m apart); (D) location of the cross-shore transects used for calculations. The width of dune front corresponds to the horizontal distance between the dune toe and the dune crest. Missing transects are due to the presence of World War II bunkers in the foredune front.

*Dune Dewulf*, and to some extent along the meso-stable *Dune Marchand*, where the dune front can be only a few meters wide, compared to the prograding *Dune du Perroquet* where the dune front width mostly ranges from 25 to 35 m (Figure 3B). The volume of the dune front varies alongshore as a function of these variations in dune height and foredune width, the largest dune volume being observed in the *Dune du Perroquet* (mean  $V_{\text{Dune}}$ :  $68.0 \text{ m}^3 \text{ m}^{-1}$ ), the mean dune volume in the *Dune Marchand* and in the *Dune Dewulf* being  $41.2 \text{ m}^3 \text{ m}^{-1}$  and  $51.5 \text{ m}^3 \text{ m}^{-1}$  respectively (Figure 3C).

Except for episodic storm events, the coast is exposed to low-energy waves. The dominant winds are from west to southwest, with a secondary wind direction from north to northeast (Figure 1). Winds are usually moderate, with more than 45 % of winds having a mean velocity of less than  $5 \text{ m s}^{-1}$ . Associated with this wind regime, waves predominantly come from the English Channel with a direction from southwest to west, followed by waves generated in the North Sea from the north to northeast. Modal significant wave height is less than 1 m with wave periods typically ranging from 4 to 8 s, but maximum wave height may episodically exceed 4 m with periods of 9 to 10 s during major storms (Ruz, Héquette, and Maspataud, 2009). Wave heights are significantly lower at the coast, due to significant shoaling and energy dissipation over the offshore sand banks, resulting in wave heights that hardly exceed 1 m in the intertidal zone even during storms (Héquette *et al.*, 2009; Héquette and Cartier, 2016).

The tidal regime in the region is semi-diurnal and is macrotidal, the tidal range reaching 5.6 m at Dunkirk during spring tides. Due to this large tidal range and current funnelling through the Dover Strait, tidal currents are powerful along the northern coast of France, with near-surface velocities up to  $1.5 \text{ m s}^{-1}$  during flood and  $1.35 \text{ m s}^{-1}$  during ebb in the narrow channels of the nearshore sand banks (Augris, Clabaut, and Vicaire, 1990). Tidal currents flow almost parallel to the shoreline, with flood currents directed to the east-northeast and ebb currents to the west-southwest. Because the dominant waves come from the southwest and the tidal currents asymmetry is flood-dominated, net sediment transport is directed to the east-northeast on the shoreface (Héquette, Hemdane, and Anthony, 2008a) and on the foreshore (Cartier and Héquette, 2011). At low tide, the beach east of Dunkirk is 400 to 500 m wide and has a very gentle gradient ( $\tan\beta = 0.01$ ). The beach consists of fine homogeneous well-sorted sands and is characterised by a series of shore-parallel intertidal bars and troughs (Cartier and Héquette, 2013).

## METHODS

### Upper Beach-dune Topographic Data

High-resolution topographic data of the coastal zone were obtained from airborne LiDAR surveys carried out from 2008 to 2016 (May 2008, March 2011, September 2011, November 2012, December 2013-January 2014, and May 2016). The 2008 survey was carried out with an Optech ALTM 1020 LiDAR having a planimetric position accuracy of  $\pm 0.25 \text{ m}$  and a vertical accuracy of  $\pm 0.1 \text{ m}$  over bare surface areas. The other surveys were conducted using a Leica ALS60 LiDAR system that acquired topographic data with a planimetric accuracy  $< \pm 0.17 \text{ m}$  and a vertical accuracy  $< \pm 0.1 \text{ m}$  as verified by several ground control points using a very high resolution differential GPS (Levoy *et al.*, 2013). Because the presence of dense and/or high vegetation on

coastal dunes (*e.g.*, sea buckthorn) can induce large vertical error range of surface elevation (Doyle and Woodroffe, 2018; Saye *et al.*, 2005), we limited our analyses to the bare upper beach and dune front up to the dune crest in order to exclude areas of dense vegetation cover that can induce significant errors ( $> 0.5 \text{ m}$ ) between the surface elevation measured by airborne LiDAR and the actual altitude of the dune surface as verified in the field with a high resolution differential GPS (Leica TPS Syst 1200, see below).

A density of data points of 1.2 to 1.4 points/ $\text{m}^2$  was obtained during the different LiDAR surveys. LiDAR topographic data were filtered to remove vegetation, buildings and other objects. Filtered data were then used to create Digital Elevation Models (DEM) using Golden Software Surfer<sup>TM</sup>. The DEMs were obtained by linear interpolation using a Delaunay triangulation resulting in a grid with a 1 m resolution, a grid cell resolution of  $1 \text{ m}^2$  appearing to provide reliable representation of topography and accurate volumetric measurements in coastal dunes using LiDAR data (Woolard and Colby, 2002). The DEMs were used to calculate sediment volume change in the coastal dunes and on the upper beach with an error range estimated to  $\pm 0.1 \text{ m}^3 \text{ m}^{-2}$ . The lower (seaward) limit of the upper beach corresponds to the mean high water level (MHW = 5.52 m), whereas the limit between the upper beach and the dune toe was determined from each DEM based on a change in slope gradient on the upper beach calculated as:

$$\|\vec{g}\| = \sqrt{\left(\frac{\partial z}{\partial x}\right)^2 + \left(\frac{\partial z}{\partial y}\right)^2} \quad (1)$$

where  $\|\vec{g}\|$  is the slope gradient,  $z$  the elevation,  $x$  and  $y$  the coordinates of each point of the calculation of the grid. The transition between the upper beach and the coastal dunes generally corresponds to a sharp increase in the value of the slope gradient that is then selected for mapping shoreline position. To validate this semi-automatic shoreline extraction method, shoreline positions detected from LiDAR data were compared at several sites of the coast of northern France with the position of the dune toe simultaneously determined in the field using a high-resolution differential GPS, which revealed small position differences between the two methods, especially along erosive shoreline stretches, with a mean standard deviation of approximately 1.5 m (Crapoulet *et al.*, 2014).

In addition to the LiDAR elevation data, *in situ* topographic profiles of the dune front and upper beach were measured along two shore-perpendicular transects (Figure 2) using a high-resolution differential GPS (Leica TPS Syst 1200) with vertical and horizontal accuracy of  $\pm 2.5 \text{ cm}$  and  $\pm 1.5 \text{ cm}$  respectively. A total of 45 topographic profiles were measured at the location of transect 1 (*Dune Dewulf*) from February 2007 to October 2016, whereas 26 profiles were measured at the location of transect 2 (*Dune du Perroquet*) from November 2007 to May 2016 (including topographic profiles extracted from the LiDAR DEMs), which allowed to calculate volume changes on the upper beach and in the coastal dunes between successive topographic surveys. For these calculations, the seaward and landward limits of the upper beach were considered as the positions of the mean high water level (MHW) and of the dune toe respectively, similarly to the method used for the LiDAR data. In the same way,

coastal dune volume changes were calculated from the dune toe to the dune crest.

### Hydro-meteorological Data

Hourly water levels recorded at the Dunkirk tide gauge station were used for distinguishing periods during which water level (WL) potentially reached the upper beach (WL > MHW) or the coastal dunes (WL > Highest Astronomical Tide level (HAT = 6.48 m)).

Analyses of offshore wave data measured at the Westhinder buoy in 27 m water depth, approximately 40 km seaward of the East Dunkirk site (Figure 1), were also carried out to discriminate stormy events that may have caused erosion on the coast of northern France. A threshold for stormy events was determined based on the frequency distribution of offshore significant wave heights ( $H_s$ ) measured at 30 minute intervals from 1997 to 2017 at the Westhinder wave buoy. Following Masselink *et al.* (2014) and Castelle *et al.* (2015), a threshold corresponding to the 95<sup>th</sup> percentile of offshore significant wave height ( $H_{s,95\%} = 2.26$  m) was used for distinguishing stormy events. A single storm event was defined as a period of  $H_s > H_{s,95\%}$  during at least 6 consecutive hours to account for the impact of tide (1/2 of a 12 h tidal cycle). In addition, we also considered that the end of a storm event occurred when  $H_s$  fell below this threshold for 6 consecutive hours.

$H_s$  recorded at the Westhinder wave buoy were also used for estimating the potential impact of waves on upper beach and coastal dunes during the period of topographic surveys (February 2007 to October 2016) through the calculation of wave energy density ( $E$ ):

$$E = \frac{1}{16} \rho g H_s^2 \quad (2)$$

and wave energy density of storm waves ( $E_s$ ):

$$E_s = \frac{1}{16} \rho g H_{s>H_{95\%}}^2 \quad (3)$$

where  $\rho$  is the density of seawater;  $g$  is the acceleration of gravity,  $H_s$  corresponds to the bihourly values of offshore significant wave height, and  $H_{s>H_{95\%}}$  is the significant wave height above the  $H_{s,95\%}$  threshold.

In order to discriminate the periods of time during which the upper beach or the coastal dunes could have been impacted by waves, wave data were filtered for retaining only waves that occurred when WL was above MHW and HAT respectively. It has to be noted that these water level threshold values represent minimum water levels recorded at the tide gauge station in Dunkirk port and that water levels on the studied beach were almost certainly higher due to wave run-up. The filtered wave data were used to compute the cumulative wave energy density ( $\sum E$ ) between consecutive beach surveys according to the following formula:

$$\sum E = \sum \frac{1}{16} \rho g H_s^2 \quad (4)$$

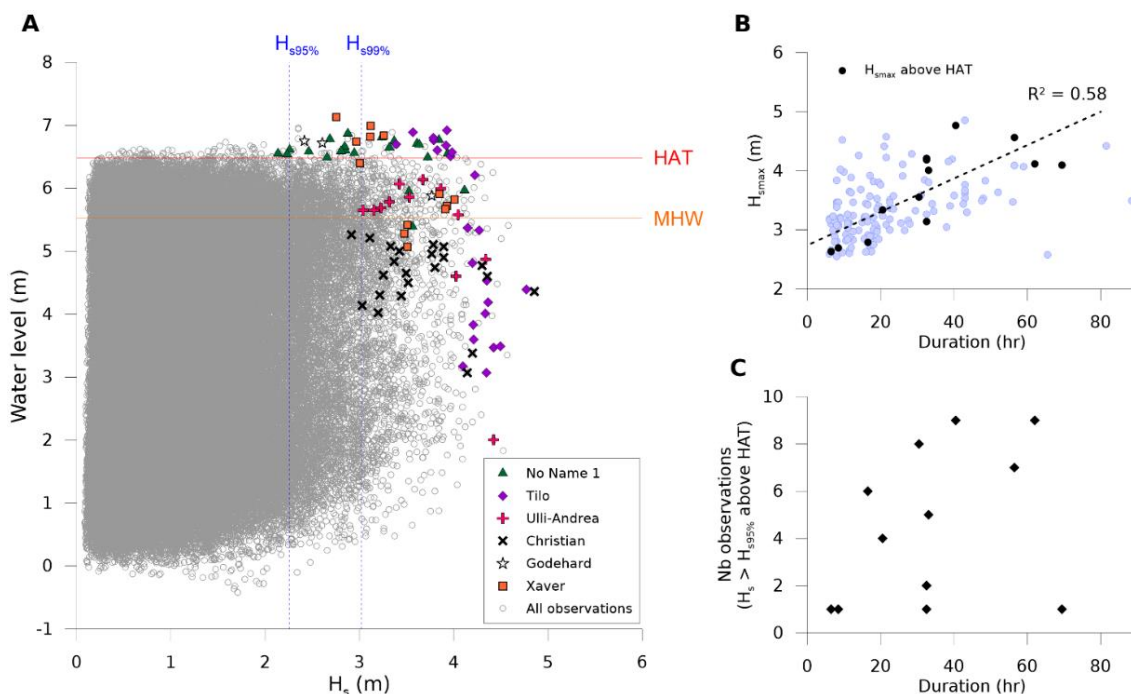


Figure 4. (A) Bi-variate plot of water levels (above Hydrographic Datum) and offshore significant wave height ( $H_s$ ) recorded simultaneously at the Dunkirk tide gauge station and at the Westhinder wave buoy between February 2007 and November 2016 (HAT: highest astronomical tide level; MHW: mean high water level); (B) Relationship between storm event duration and maximum significant wave height ( $H_{s,max}$ ), the black dots correspond to storm events during which WL > HAT; (C) Relationship between storm event duration and number of observations of  $H_s > H_{s,95\%}$  above HAT.

Unfortunately, the offshore wave data from February 2007 to October 2016 are not complete with about 11% of missing data, but most of the missing data correspond to non-storm conditions. Analyses of wind forcing conditions that may potentially lead to onshore aeolian sand transport and coastal dune development were carried out using hourly mean wind speed measured at the Météo-France weather station in Dunkirk. The potential dune growth or post-storm dune recovery was assessed by computing the number of hourly observations of onshore-directed winds (+90° to -90° relative to shore-normal) with speeds > 5 m s<sup>-1</sup>, which corresponds to a minimum aeolian threshold velocity for the transport of fine sand (Bagnold, 1941; Davidson-Arnott and Bauer, 2009). Because a number of previous studies showed that aeolian sediment flux is typically proportional to the cube of wind speed (*e.g.*, Davidson-Arnott, MacQuarrie, and Aagaard, 2005; Dong *et al.*, 2003; Lettau and Lettau, 1978), we estimated the magnitude of sand transport from the upper beach to the dune between successive surveys using a cumulative aeolian transport index ( $\Sigma W$ ) in the form of:

$$\Sigma W = \Sigma W_{cr < MHWs}^3 \quad (5)$$

where  $W_{cr < MHWs}$  is the mean hourly wind speed above 5 m s<sup>-1</sup> recorded when WL was lower than the mean high water spring tide level (MHWS). Wind records were excluded when water level was above MHWS, because onshore aeolian transport is restricted during high water levels that partially or totally limit cross-shore aeolian fetch length (Ruz and Meur-Férec, 2004; Bauer *et al.*, 2009). In addition, in order to investigate only post-storm dune recovery processes between successive topographic surveys without the influence of possible erosional episodes, the periods during which WL exceeded HAT between two successive surveys were eliminated in some of these analyses.

## RESULTS

### Storm Events from 2007 to 2016

A total of 147 storm events occurred between 22 February 2007 and 1 October 2016 (first and last dates of profile surveying) when using a 95<sup>th</sup> percentile wave height threshold (Figures 4B and 5A). Storm events mostly occurred during fall-winter periods, the occurrences of  $H_s > H_{s95\%}$  being much lower during the summer months (Figure 5A). Several of these events were characterized

by maximum offshore  $H_s$  that largely exceeding the 99<sup>th</sup> percentile wave height (3.02 m) (Figure 4A), but these high amplitude waves did not necessarily impact the coastal dunes or the upper beach because they did not occur at or near high tide or because of neap tide conditions. This was the case during storm Ulli, in early January 2012, for example, during which  $H_s$  reached 4.42 m (Figure 6A), but several hours before high tide when water level was only 2.0 m above Hydrographic Datum (Table 1; Figure 4A). Similarly, during the heavy storm Christian in late October 2013 a maximum offshore  $H_s$  of 4.85 m was observed (Table 1, Figure 6A), but this storm is thought to have had no effects on the dunes because it occurred during a neap tide (Figure 6C), which prevented the upper beach to be reached by waves (Figure 6D). When considering only the stormy events during which the water level exceeded HAT, a total of only 12 events occurred during the study period (Figure 4B), because the other storm events either took place during a neap tide or peaked several hours before or after high tide.

Storms were also variable in strength and duration during the studied period, longer storms being generally associated with higher maximum  $H_s$  and higher occurrences of  $H_s > H_{s95\%}$  above HAT (Figure 4B,C). The year 2007 stands out with several long-lasting storms, notably in March and November (Table 1), which potentially allowed the waves to reach the dune toe during several successive high tides. This explains the high number of monthly occurrences of storm waves ( $H_s > 95^{\text{th}}$  percentile wave height) above HAT in March and November (Figure 5C). Not only the frequency of storm waves was high during these storms, but the total wave energy was also remarkably high during these events. Comparatively, the series of storms that hit western Europe in the fall and winter of 2013-2014 resulted in a smaller number of high water levels above HAT and were associated with smaller waves of lower energy (Figure 5C), except during a storm on 10-11 October (No Name 5, Table 1) when an offshore  $H_s$  of 3.9 m (Figure 6A), corresponding to a wave energy density of nearly  $10 \times 10^3 \text{ J m}^{-2}$ , was recorded when the water level was significantly higher than HAT (Figure 6D). Although the series of storms of fall-winter 2013-2014 did not produce a particularly large number of high water levels above HAT (Figure 5B), they have been responsible for extreme water levels largely above HAT,

Table 1. Major storms that hit the coast of northern France between February 2007 and October 2016. Nb  $H_s > H_{s95\%}$  corresponds to the number of bihourly observations of offshore  $H_s$  above the 95<sup>th</sup> percentile wave height threshold during a storm;  $WL_{\max}$  and  $H_{s\max}$  correspond respectively to the maximum water level and maximum  $H_s$  reached during a storm;  $H_s$  at  $WL_{\max}$  is the  $H_s$  when the maximum water level was reached during a storm, and  $WL$  at  $H_{s\max}$  corresponds to the water level when the maximum  $H_s$  was recorded (numbers in bold characters indicate storms during which WL was above MHW when  $H_{s\max}$  was recorded).  $H_s$  and WL were recorded at the Westhinder wave buoy and Dunkirk tide gauge respectively (see Figure 1 for location).

Storm name	Dates	Nb $H_s > H_{s95\%}$	$WL_{\max}$ (m above HD)	$H_{s\max}$ (m)	$H_s$ at $WL_{\max}$ (m)	$WL$ at $H_{s\max}$ (m above HD)
No Name 1	17-21 March 2007	142	6.87	4.12	2.88	<b>5.97</b>
Tilo	9-10 November 2007	81	6.92	4.77	3.93	4.39
No Name 2	10-12 March 2008	109	6.58	4.09	2.79	1.70
No Name 3	20-22 March 2008	105	6.74	4.57	3.09	3.35
No Name 4	8-9 December 2011	52	6.56	4.21	2.68	4.85
Ulli-Andrea	3-6 January 2012	144	6.14	4.42	3.67	2.00
No Name 5	10-11 October 2013	62	6.70	4.19	3.90	<b>5.82</b>
Christian	27-28 October 2013	69	5.26	4.85	2.91	4.36
Godehard	2-6 November 2013	57	6.59	3.77	2.27	<b>5.88</b>
Xaver	5-6 December 2013	46	7.13	4.01	2.75	<b>5.82</b>

especially during storm Xaver during which the water level exceeded the 100-year return period water elevation on 6 December 2013 at Dunkirk (Figure 6D) due to a storm surge of 1.26 m at high tide combined with a spring tide (Daubord, 2014).

### Storm Impacts and Beach-dune Recovery

#### Upper Beach/dune Evolution at the Dune Dewulf

The beach and dune profile monitoring carried out at the *Dune Dewulf* site from February 2007 to December 2016 shows several phases of erosion and accumulation on the backshore (Figure 7D). The foredune and upper beach experienced significant erosion in response to the storm of 17-21 March 2007 (No Name 1), which was characterized by a large number of observations of high

energy waves  $>$  HAT (Figure 5C). The topographic profile surveyed on 22 March 2007, only a few days after the storm, shows a flattening of the upper beach and a retreat of the dune toe of about 4 m (Figure 7B), corresponding to a loss of about  $8.1 \text{ m}^3 \text{ m}^{-1}$  in the dune and  $4.4 \text{ m}^3 \text{ m}^{-1}$  on the upper beach (Figure 7D) when compared with the pre-storm profile surveyed on 22 February 2007 (Figure 7B). A following topographic survey in early October 2007 revealed that the upper beach totally recovered from erosion with a sediment volume exceeding its initial volume, but that the coastal dune front only partly recovered to its pre-storm sediment volume (Figure 7D,E).

The following storm Tilo that struck the coast of northern France on 9 and 10 November 2007 (Table 1) also had an impact

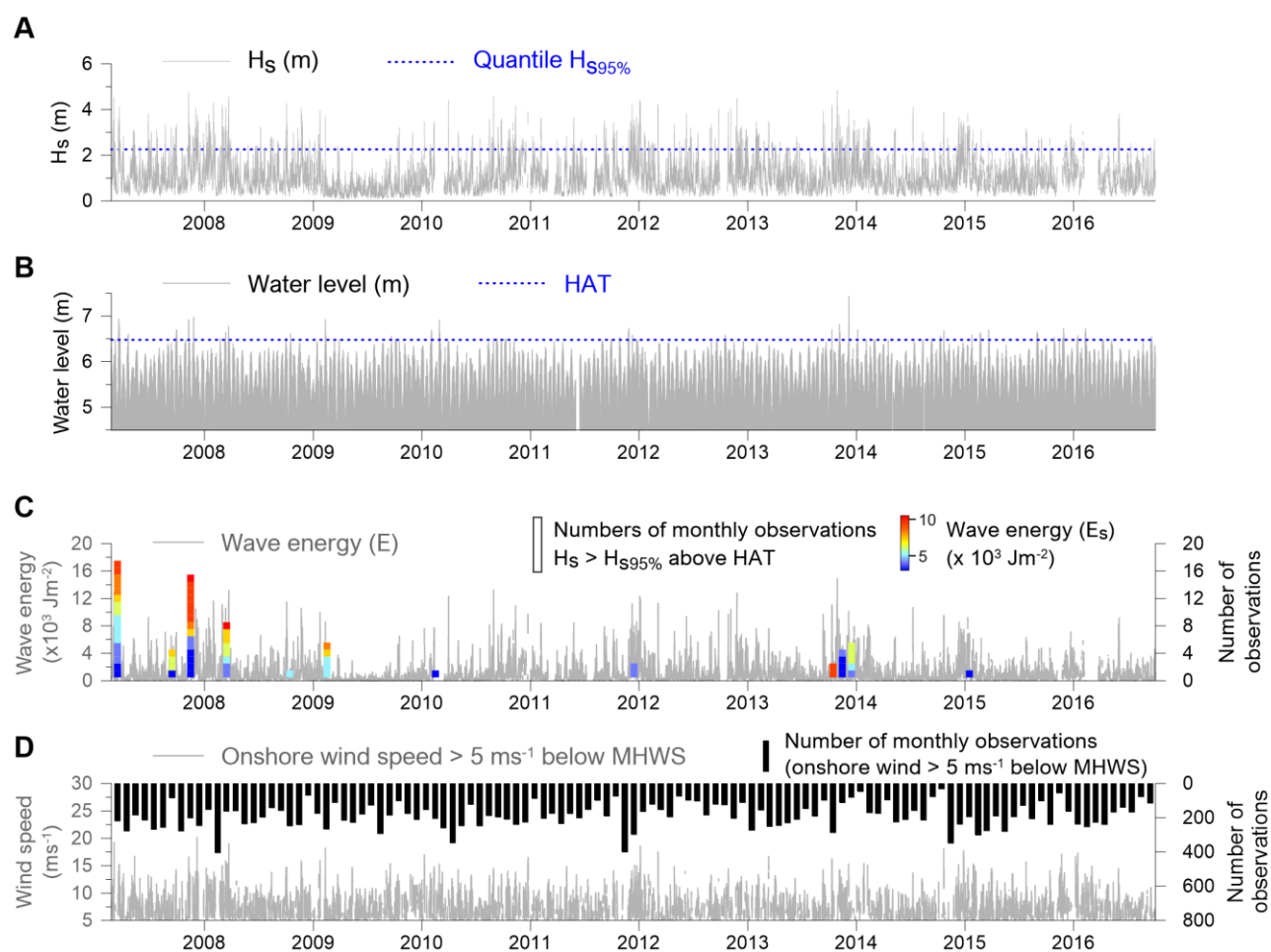


Figure 5. Time series of offshore significant wave height, wave energy density, water level and wind speed measured between 22 February 2007 and 1 November 2016. (A) Offshore significant wave height ( $H_s$ ) recorded at the Westhinder buoy (see Figure 1 for location); (B) water level (WL) above Hydrographic Datum recorded at the Dunkirk tide gauge; (C) Wave energy density ( $E_s$ ) computed for all offshore waves (light grey lines), monthly frequency of observations of  $H_s > H_{s95\%}$  that occurred when WL was above highest astronomical tide (HAT) (vertical bars) and wave energy density of storm waves ( $E_s$ ) computed for  $H_s > H_{s95\%}$  above HAT (colored bars); (D) Time series (light grey lines) and monthly frequency (vertical black bars) of onshore-directed wind speeds  $> 5 \text{ m s}^{-1}$  recorded at the Meteo-France weather station in Dunkirk when WL was below mean high water spring tide level (MHWS).

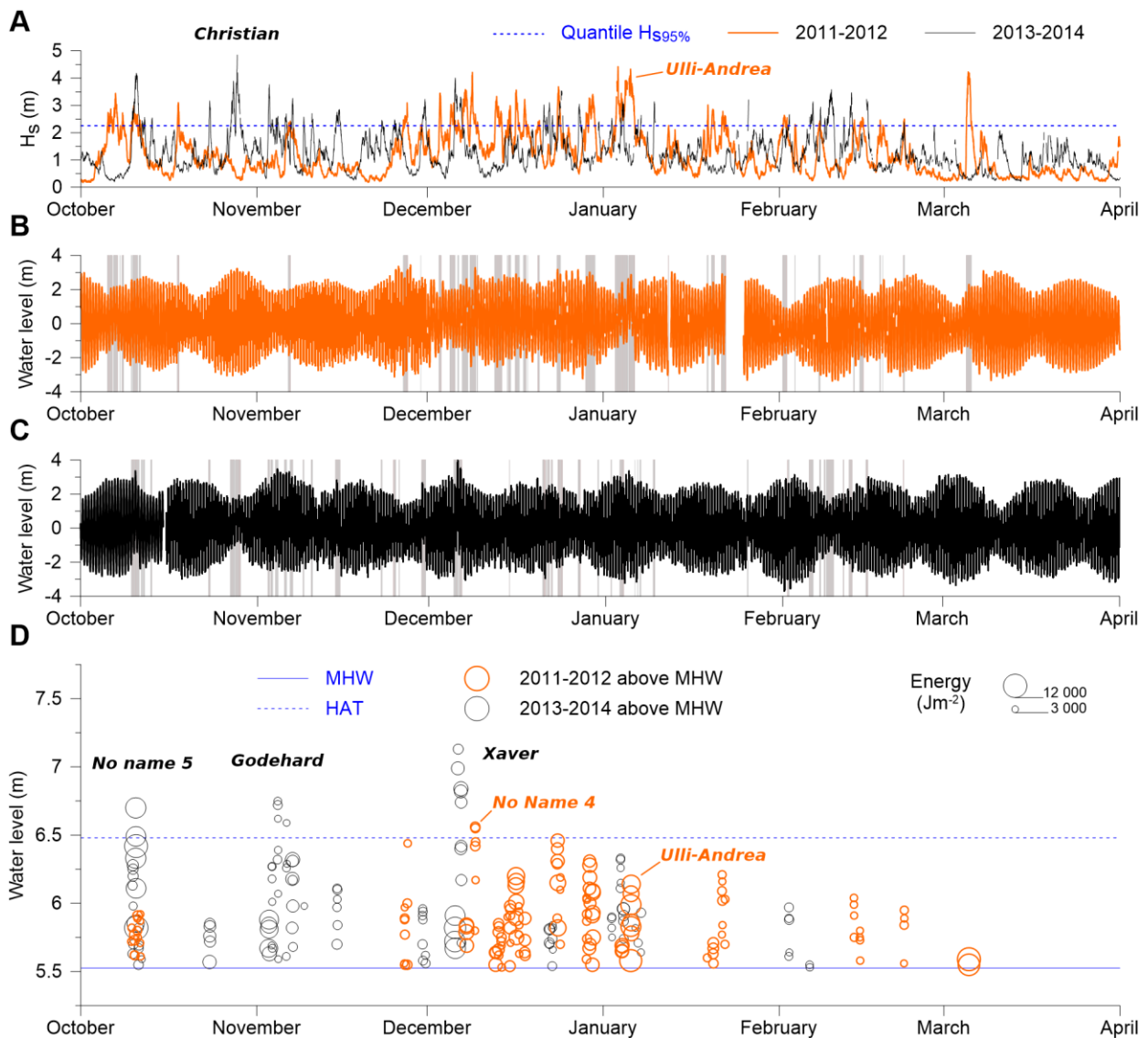


Figure 6. Times series of (A) offshore significant wave height ( $H_s$ ) recorded at the Westhinder buoy (see Figure 1 for location) during fall-winter 2011-2012 and 2013-2014, water level recorded at the Dunkirk tide gauge during (B) fall-winter 2011-2012 and (C) 2013-2014, (D) wave energy density of storm waves ( $H_s > H_{s95\%}$ ) that occurred above mean high water level (MHW) during fall-winter 2011-2012 and 2013-2014. The shaded vertical bars in (B) and (C) correspond to periods during which  $H_s > H_{s95\%}$ .

on the foredune evidenced by an erosion of nearly  $4 \text{ m}^3 \text{ m}^{-1}$  measured on the surveyed profile four days after the storm (Figure 7D), due to high  $H_s$  ( $H_{smax} = 4.77 \text{ m}$ ), and extreme water levels up to  $6.92 \text{ m}$  (Table 1; Figure 5B), which corresponds to  $0.44 \text{ m}$  above HAT. It is noteworthy that significant sediment accumulation was measured on the upper beach ( $\approx 14 \text{ m}^3 \text{ m}^{-1}$ ) following this storm, which may be partly due to the deposition of sand eroded from the dune front. This event was followed by several stormy events during the rest of November, some of them being characterized by high water levels above HAT but with moderate  $H_s$  ( $2.3 \text{ m} < H_s < 2.6 \text{ m}$ ) or by higher waves ( $H_s > H_{s99\%}$ )

associated with water levels that only reached the upper beach (i.e.,  $\text{MHW} < \text{WL} < \text{HAT}$ ). This can explain the modest erosion of the coastal dune front ( $-1.9 \text{ m}^3 \text{ m}^{-1}$ ) and the more significant erosion of the upper beach ( $-13.1 \text{ m}^3 \text{ m}^{-1}$ ) measured in early December 2007 (Figure 7D).

The beginning of 2008 was also marked by a series of storm events, especially in March when two successive events with  $H_{smax}$  of  $4.09 \text{ m}$  and  $4.57 \text{ m}$  took place, associated with high WL that reached respectively  $6.58 \text{ m}$  and  $6.74 \text{ m}$  above HD (Table 1), which resulted in relatively high wave energy density values for that particular month (Figure 5C). As a result, the dune and

especially the upper beach experienced erosion as shown by the profile surveyed in early April 2008 (Figure 7D). For the remaining of 2008, the upper beach showed successive phases of sediment accumulation whereas the dune underwent slight erosion followed by slow and moderate recovery.

Our measurements from January 2009 to January 2012 revealed alternating phases of erosion and accretion, with some noticeable dune and upper beach erosion (Figure 7D) due to the impacts of a few significant storm events such as storm Quentin in February 2009 (Figure 5C), storm No Name 4 of 8-9 December 2011 or storm Ulli-Andrea that hit the coast from 3 to 6 January 2012 (Figure 6D). However, this period was overall characterized by a quasi-absence of high energy events during which water

levels exceeded HAT (Figure 5C), which is why the upper beach underwent severe erosion during that time interval (Figure 7 D,E). Nevertheless, coastal dune erosion was rather limited (Figure 7D) and the dune front even slightly recovered until September 2011 (Figure 7E) which may have been favored by a high frequency of onshore-blowing winds above  $5 \text{ m s}^{-1}$  (Figure 5D) that could have been responsible for onshore aeolian sand transport from the beach to the dunes. From late January 2012 to February 2013, the cumulative volume change of the upper beach and coastal dune shows a clear accretionary trend, especially in the dune (Figures 7 D,E). This period was characterized by an absence of high water levels  $> \text{HAT}$  (Figure 5B,C) which prevented wave scarping of the dune toe. Sand accumulation on the dune front resulted in

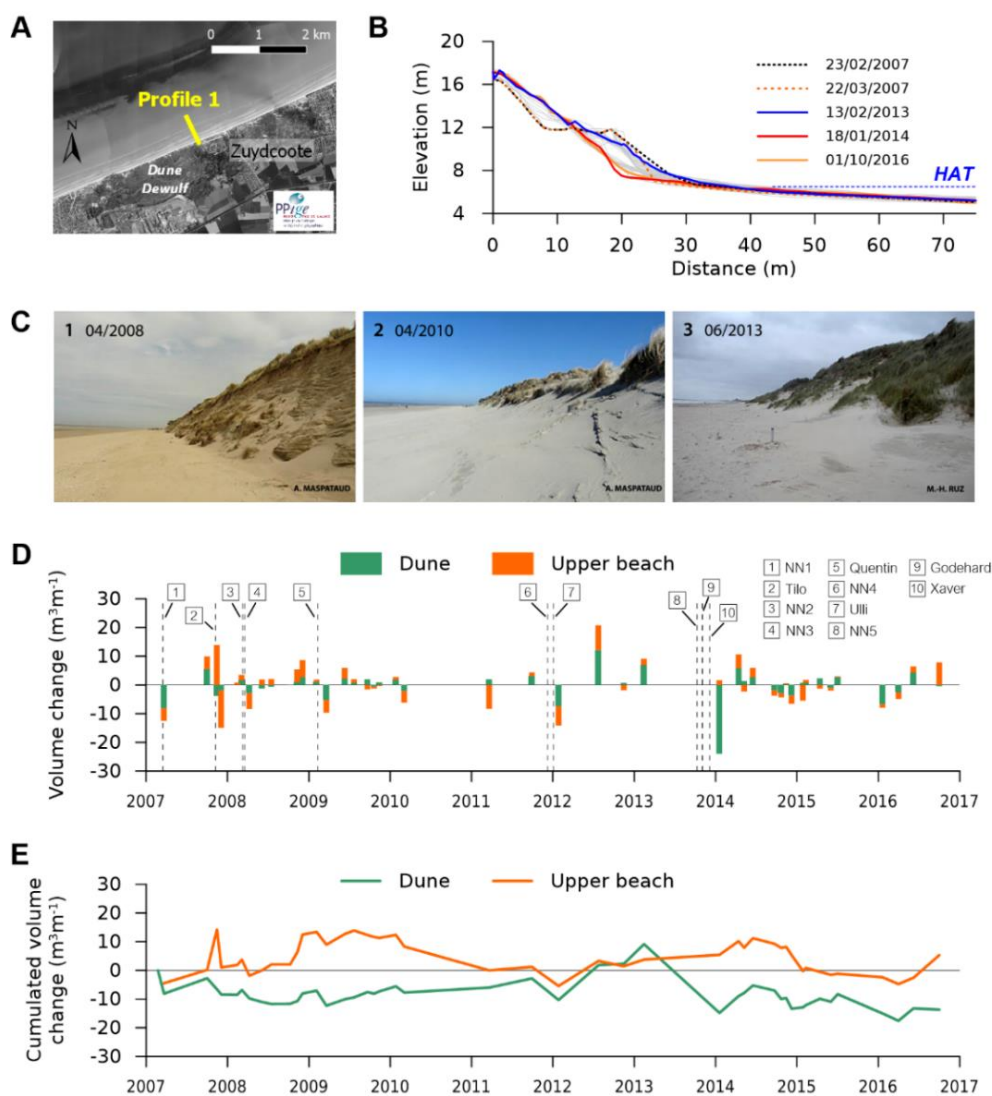


Figure 7. (A) Aerial photograph showing the location of topographic profile 1 at the *Dune Dewulf* (elevations are in m above Hydrographic Datum); (B) Envelope of beach and dune profile variations between 22 February 2007 and 1 October 2016 (the colored profiles correspond to selected profiles after major events); (C) ground photographs showing phases of coastal dune recovery at the location of profile 1 from April 2008 to June 2013; (D) coastal dune and upper beach volume change based on elevation variations measured along profile 1 between 22 February 2007 and 1 October 2016; (E) cumulative dune and upper beach volume change along profile 1.

February 2013 in a nearly full recovery to its initial state of February 2007 (Figure 7B) and in vertical dune growth upslope, which explains the observed increase in cumulated dune volume (Figure 7E). The dune front was stabilized by vegetation (*Elymus farctus* and *Ammophila arenaria*) (Figure 7C3) which favored further aeolian sand accumulation on the stoss side of the dune.

This relatively calm period was followed by the unusual series of closely spaced storms of fall-winter 2013-2014. For most of them, these storms have not resulted in exceptionally high wave energy at high tide on the coast of northern France (Figures 5C and 6D), but as mentioned earlier they induced remarkably high water levels, especially during storm Xaver in early December 2013 (Figure 6D). The unusual character of this sequence of storms is obvious when compared with the fall and winter of 2011-2012, for example, when only two observations of storm wave ( $H_s > H_{s,95\%}$ ) were recorded above HAT (cf., storm No Name 4, Figure 6D). As a consequence, the cumulative impacts of the storms of fall and early winter 2013-2014 caused major dune front erosion, with a retreat of about 8 m of the dune toe, as revealed by the topographic profile surveyed on 18 January 2014 (Figure 7B,D). Although the coastal dune partially recovered from storm erosion during the first few months of 2014 (Figure 7D,E), our subsequent measurements showed that the dune continued to erode and hardly recovered during the following two years (Figure 7 D,E) despite a virtual absence of high energy events associated with high water levels (Figure 5C) and a high frequency of onshore winds favorable to sand accumulation on the dune front (Figure 5D).

Cumulative volume change of the upper beach from February 2007 to October 2016 clearly shows that the upper beach is characterized by significant volume fluctuations and can rapidly gain sediment after erosion events, whereas the coastal dune recovers more progressively over longer time periods (Figure 7E). Our results also show that after the series of high-energy eroding storms that occurred from early 2007 to early 2009 (Figure 5C), slow but almost continuous coastal dune recovery took place during the following four years (Figure 7 C,E), but that after the series of storms of 2013-2014, the coastal dune was unable to recover to its initial state at that location (Figure 7E), possibly because of the massive erosion caused by these storm events.

#### Upper Beach/dune Evolution at the Dune du Perroquet

Conversely to what was observed at the *Dune Dewulf* (Figure 7), our measurements across the foredune and upper beach at the *Dune du Perroquet* revealed an almost continuous upper beach accretion and coastal dune development between November 2007 and May 2016 (Figure 8 B,E). Although some erosion of the upper beach and/or the coastal dune was observed on a few occasions (Figure 8D), a gain of approximately  $20 \text{ m}^3 \text{ m}^{-1}$  on the upper beach and  $70 \text{ m}^3 \text{ m}^{-1}$  in the coastal dune was measured during the survey period (Figure 8E). Compared to the *Dune Dewulf* site, coastal dune erosion has been very sporadic and generally moderate at the *Dune du Perroquet*. Virtually no dune erosion was observed until the end of 2011 even if several significant storms occurred in late 2007 and in 2008 (Figure 5, Table 1), which resulted in the erosion of the coastal dune at the *Dune Dewulf* site on several occasions (Figure 7D). Even storms No Name 5 and Godehard in the fall of 2013 did not induce any

beach or dune erosion (Figure 8D) although WL largely exceeded HAT (Table 1). A maximum eroded volume of  $-6.1 \text{ m}^3 \text{ m}^{-1}$  was recorded on 9 December 2013 (Figure 8D) due to scarping of the dune front (Figure 8B) that occurred a few days before during storm Xaver. The following topographic survey on January 2014 showed slight accumulation on the upper beach, but no change in the coastal dune (Figure 8D). However, after 18 months the coastal dune has fully recovered owing to an accretion of  $11.7 \text{ m}^3 \text{ m}^{-1}$  (Figure 8D). Not only the coastal dune experienced post-storm recovery during that period, but it continued to develop upward and seaward (Figure 8E).

#### Analyses of Hydro-meteorological Forcing on Coastal Dune Volume Change

Analysis of dune volume change ( $\Delta V_{\text{Dune}}$ ) at the *Dune Dewulf* site as a function of cumulative wave energy density ( $\sum E$ ) between consecutive surveys expectedly showed that eroded dune volumes increase with total wave energy above a water level threshold, the largest eroded volume ( $24.1 \text{ m}^3 \text{ m}^{-1}$ ) having been measured after the series of storms of the fall and early winter of 2013-2014 (Figure 9A). A significantly better relationship was found when using a WL threshold at MHW ( $r^2 = 0.72$ ) compared to the correlation coefficient obtained with a threshold at HAT ( $r^2 = 0.27$ ), notably because mild erosion occurred during some periods during which HAT was not exceeded, resulting in  $\sum E = 0$  in these cases. This shows that erosion could take place at this site even when  $WL < HAT$  because the dune toe could be reached and eroded by waves due to wave run-up. It is noteworthy that consecutive surveys were sometimes separated by fairly long period of times during which some erosion and/or accumulation may have taken place without having been measured, which probably reduced the degree of correlation obtained between  $\Delta V_{\text{Dune}}$  and  $\sum E$ . Another factor that may also affect the degree of correlation between these variables is offshore wave direction that may result in variable impacts at the coast (for similar wave energy levels).

No analysis of dune volume change ( $\Delta V_{\text{Dune}}$ ) as a function of wave energy density ( $\sum E$ ) could be carried out at the *Dune du Perroquet* site due to the limited number of dune erosion observations (Figure 8D). The coastal dune at this site was less impacted by waves during storms because the elevation of the dune toe is higher than to the west (Figure 10A). In addition, the upper beach is wider at the base of the *Dune du Perroquet* (Figure 10B), which enhances wave energy dissipation and reduces the impact of waves on coastal dunes.

The analysis of the relationship between dune volume change ( $\Delta V_{\text{Dune}}$ ) and potential sand transport from the beach to the dune, through the use of a cumulative aeolian transport index ( $\sum W$ ), revealed weak correlations at the *Dune Dewulf* site (Figure 9B), even when excluding periods between successive surveys during which  $WL > HAT$  that potentially resulted in significant coastal dune erosion ( $r^2 = 0.38$ ). This result suggests that post-storm dune recovery is not simply a function of the frequency of onshore-directed winds above threshold of sediment motion ( $> 5 \text{ m s}^{-1}$ ), but that other factors favor or limit aeolian sediment flux to the coastal dunes. In addition to surface moisture that may vary with rainfall and/or tides on these beaches, the width of the upper beach can represent a major factor controlling wind fetch and thus

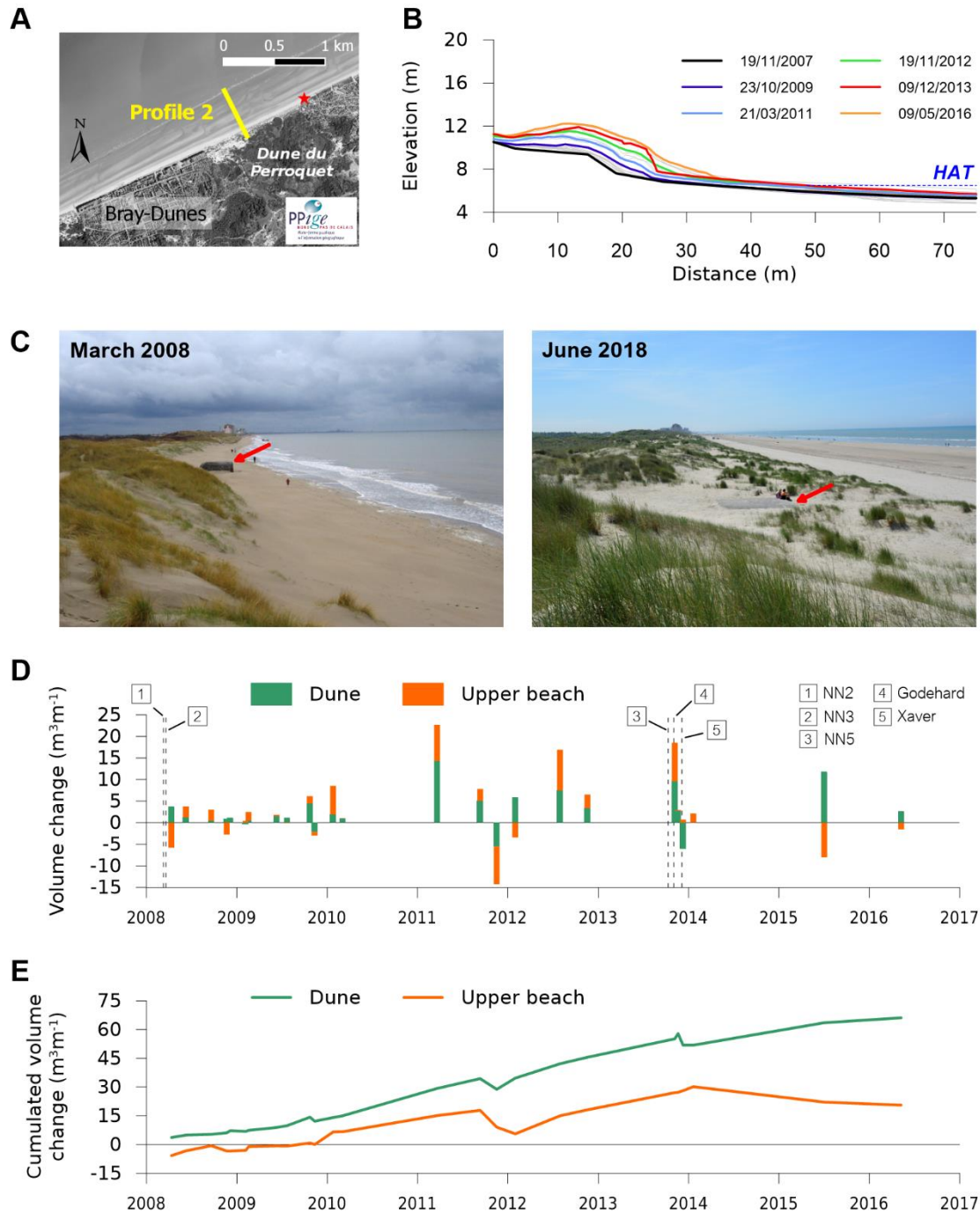


Figure 8. (A) Aerial photograph showing the location of topographic profile 2 at the *Dune du Perroquet* (elevations are in m above Hydrographic Datum), the star indicates the location of the bunker shown in photographs (C); (B) Envelope of beach and dune profile variations between 19 November 2007 and 9 May 2016 (the colored profiles show phases of accretion of the coastal dune and upper beach); (C) ground photographs showing sand accumulation and coastal dune development between March 2008 and June 2018 at the front of the *Dune du Perroquet* (the arrows point to a bunker that has been almost completely buried by sand due to incipient foredune growth); (D) coastal dune and upper beach volume change based on elevation variations measured along profile 2 between 19 November 2007 and 9 May 2016; (E) cumulative dune and upper beach volume change along profile 2.

aeolian transport rates (Anthony, Ruz, and Vanh e, 2009; Bauer and Davidson-Arnott, 2003; Ruz and Meur-Ferec, 2004).

In comparison, a much better correlation was obtained between dune volume change and cumulative aeolian transport index ( $\Sigma W$ ) ( $r^2 = 0.71$ ) at the *Dune du Perroquet* (Figure 8C). This can probably be explained by the larger width of the upper beach at the *Dune du Perroquet* compared to *Dune Dewulf* (Figure 10B). A wide upper beach would likely favor aeolian transport and possible onshore sediment transfer from the beach to dunes, whereas a narrower upper beach would restrict wind-driven dune recovery. Not only a narrower upper beach results in a shorter aeolian fetch, but it is subject to more frequent flooding at high tide, which restricts aeolian transport and thus sediment supply to the coastal dunes even during favorable wind conditions, which may explain the weak relationship found between  $\Delta V_{Dune}$  and  $\Sigma E$  at the *Dune Dewulf* site (Figure 9B).

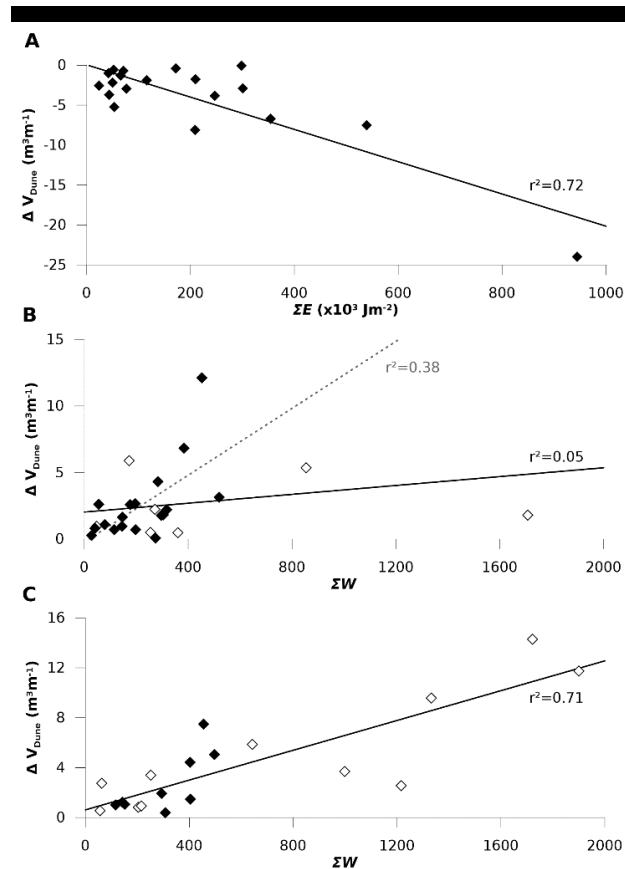


Figure 9. (A) Relationship between coastal dune volume change ( $\Delta V_{Dune}$ ) and cumulative wave energy density ( $\Sigma E$ ) when WL > MHW; (B,C) relationship between  $\Delta V_{Dune}$  and cumulative aeolian transport index ( $\Sigma W$ ) when WL < MHWS (see text for explanation). (A) and (B) represent  $\Delta V_{Dune}$  measured on profile 1 (*Dune Dewulf*), (C) represents  $\Delta V_{Dune}$  measured on profile 2 (see Figure 2 for location). Open symbols in (B) and (C) correspond to periods during which WL exceeded HAT.

**Alongshore Variability in Coastal Dune Volume Change**  
 Based on the DTMs derived from the successive LiDAR topographic surveys carried out between May 2008 and May 2016, the volume of the upper beach fluctuated during the distinct periods between each survey but overall remained remarkably

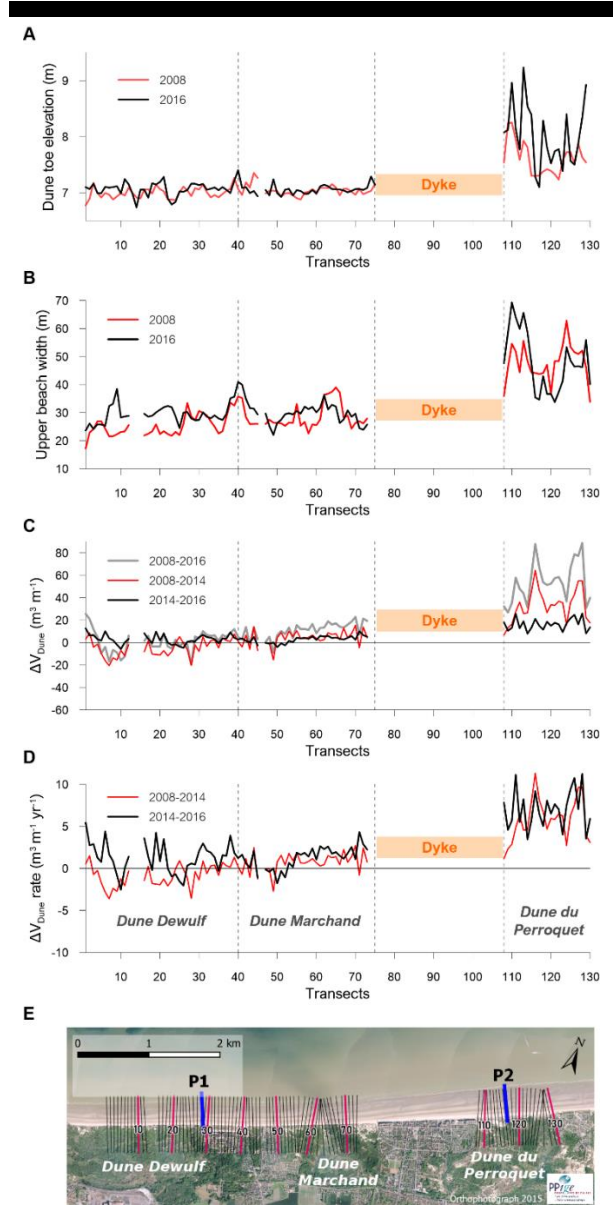


Figure 10. Longshore variations in (A) dune toe elevation, based on slope gradient change (elevations are in m above Hydrographic Datum), (B) upper beach width, (C) coastal dune volume change ( $\Sigma V_{Dune}$ ), and (D) annual rate of change of dune volume between Dunkirk and the Belgium border based on airborne LiDAR topographic data collected between May 2008 and May 2016 (measurements were carried out along cross-shore transects spaced 50 m apart); (E) location of the cross-shore transects used for calculations and of topographic profiles P1 and P2.

stable when considering the entire 2008-2016 period (Table 2). Conversely, the coastal dunes gained more than  $110 \times 10^3 \text{ m}^3$  between 2008 and 2016 even if significant erosion occurred during the 2012-2014 period with a loss of about  $72 \times 10^3 \text{ m}^3$  that can most likely be attributed to the series of storms of fall and early winter 2013-2014. Interestingly, during the 2014-2016 period that followed this series of storms, the upper beach lost approximately  $56 \times 10^3 \text{ m}^3$  whereas a similar volume of sediment was deposited in the dunes during the same time interval (Table 2), which can suggest a sediment transfer from the upper beach to the coastal dunes that were recovering through aeolian processes.

However, coastal dune erosion and post-storm recovery varied considerably from one foredune to the other. When looking at the coastal dune volume change per unit length of coastline (in order to compare foredunes with different lengths along the coast), one can see that the volume of the *Dune Dewulf* was similar in 2008 and in 2016, but that the *Dune Marchand* and especially the *Dune du Perroquet* gained sediment with an accumulation of about  $18.5 \text{ m}^3 \text{ m}^{-1}$  and  $68 \text{ m}^3 \text{ m}^{-1}$  respectively (Table 3). During all periods except the 2012-2014 time interval, the foredunes all along this coastal stretch experienced sand accumulation or were stable with a clear increase in sediment accretion eastward. During the 2012-2014 period, the *Dune Dewulf* and *Dune Marchand* underwent erosion of about  $-14.6 \text{ m}^3 \text{ m}^{-1}$  and  $-17.2 \text{ m}^3 \text{ m}^{-1}$ , but the *Dune du Perroquet* still gained some sediment (Table 3). Because the 2014 LiDAR survey was carried out shortly after storm Xaver, which was the most erosive storm event at this site (Figure 8D) because of the exceptionally high water level reached during this event (Figure 6D), this accumulation of approximately  $5.4 \text{ m}^3 \text{ m}^{-1}$  most likely corresponds to the remaining volume of pre-storm accretion rather than post-storm recovery, as shown on profile 2 (Figure 8 B,D).

The alongshore variability in foredune volume change can be analyzed in more detail when examining volume changes at transects spaced 50 m apart along the coast (Figure 10C). A positive eastward gradient in dune volume change is visible for the period 2008-2016 with some erosion in the *Dune Dewulf* followed by increasing accumulation to the east in the *Dune Marchand* up to more than  $20 \text{ m}^3 \text{ m}^{-1}$ , culminating to more than  $60 \text{ m}^3 \text{ m}^{-1}$  along large portions of the *Dune du Perroquet* foredune (Figure 10C). A west-east gradient in volume change is also obvious for the sub-periods 2008-2014 and 2014-2016. These data show that erosion during the 2008-2014 period essentially

took place along the *Dune Dewulf* shoreline while the dune front along *Dune Marchand* was largely stable or experienced slight accumulation. In comparison, the *Dune du Perroquet* was affected by significant accretion that exceeded  $40 \text{ m}^3 \text{ m}^{-1}$  in places during the same period (Figure 10C). The period 2014-2016 was dominated by sand accumulation, revealing that post-storm dune recovery was widespread after the series of storm of fall-winter 2013-2014 (Figure 10C). Because the periods of volume change measurements are of different lengths, ranging from 28 months to 8 years, annual rates of change of dune volume were computed for assessing the mean rate of change during each time period. The results of these calculations show that the *Dune Dewulf* changed from an erosion regime between 2008 and 2014 to a spatially-irregular recovery regime during the almost storm-free period 2014-2016 whereas the *Dune Marchand* and the *Dune du Perroquet* were mainly dominated by accretion during both periods (Figure 10D). The rates of change in dune volume were not only higher at the *Dune du Perroquet*, ranging from about 5 to  $10 \text{ m}^3 \text{ m}^{-1} \text{ yr}^{-1}$  compared to about 1 to  $4 \text{ m}^3 \text{ m}^{-1} \text{ yr}^{-1}$  at the *Dune Marchand*, but they were remarkably similar at any location during the different periods which suggests a fairly stable sediment supply to the dunes that continued to develop at a constant rate throughout the period 2008-2016.

Comparisons of alongshore dune volume change (Figure 10C) with dune toe elevation (Figure 10A) and with upper beach width (Figure 10B) show a strong relationship with these morphological variables. The LiDAR data revealed that both the dune toe elevation and the width of the upper beach were significantly greater along the *Dune du Perroquet* compared with the two other dune sectors where lower elevations of the dune toe and narrower upper beach widths are associated with lower rates of dune volume change (Figure 10D). These data also show that the elevation of the dune toe remained virtually the same between 2008 and 2016 along the *Dune Dewulf* and the *Dune Marchand*, but that it strongly increased at the *Dune du Perroquet* (Figure 10A) due to incipient foredune development (Figure 8C). The upper beach width also tended to increase between 2008 and 2016, but in a more irregular pattern along the coastline (Figure 10B). Our data also suggest that dune volume change was partly controlled by the initial dune and upper beach morphology, with a strong correspondence between dune front volume change from 2008 to 2016 and upper beach width measured in May 2008 (Figure 11). A somewhat weaker relationship is observed

Table 2. Sediment volume change on the upper beach and in the foredunes between Dunkirk and the Belgium border based on successive airborne topographic LiDAR surveys from May 2008 to May 2016 (see Figure 9 for location). Numbers in bold highlight erosion.

Volume change ( $\text{m}^3$ )	2008-2011	2011-2012	2012-2014	2014-2016	2008-2016
Upper beach	18 865	11 965	29 468	- 56 005	4293
Coastal dunes	100 056	32 740	- 71 195	51 628	113 230
Total	118 921	44 705	- 41 726	4376	117 523

Table 3. Sediment volume change per unit length of coastline ( $\text{m}^3 \text{ m}^{-1}$ ) in the foredunes between Dunkirk and the Belgium border based on successive airborne topographic LiDAR surveys from May 2008 to May 2016 (see Figure 9 for location). Numbers in bold highlight erosion.

Volume change ( $\text{m}^3 \text{ m}^{-1}$ )	2008-2011	2011-2012	2012-2014	2014-2016	2008-2016
<i>Dune Dewulf</i>	11.21	1.30	<b>-14.56</b>	3.06	1.01
<i>Dune Marchand</i>	19.33	7.10	<b>-17.19</b>	9.24	18.48
<i>Dune du Perroquet</i>	26.20	13.96	5.38	22.34	67.88

between dune volume change and initial dune height, the highest  $\Delta V_{\text{Dune}}$  tending to be associated with the lowest dunes located in the *Dune du Perroquet* sector (Figure 11).

### DISCUSSION

Our results show that coastal dunes located at a relatively short distance apart along a coastal stretch with the same wave exposure can have significantly different responses to storms. Not only the impacts of storm events were much greater on some dunes, but post-storm recovery also varied from one foredune to another. To the west the foredune of the *Dune Dewulf* experienced alternating phases of erosion and post-storm recovery (Figure 7D) while eastward, the foredune at the *Dune du Perroquet* was dominated by almost continuous accretion (Figure 8E). It is largely recognized that coastal dune evolution (*i.e.*, development, stability or erosion) and shoreline change are strongly controlled by beach and dune sediment budget (Hesp, 2011; Houser, Hapke, and Hamilton, 2008; Psuty, 1988). In this study, the observed alongshore variability in upper beach and foredune change can probably be explained by a sediment surplus at the eastern site due to a dominant eastward-directed sediment flux in the nearshore and intertidal zones induced by wave and tidal currents (Cartier and Héquette, 2011; Héquette, Hemdane, and Anthony, 2008b). Furthermore, on the dry upper beach the prevailing southwest to westerly winds (Figure 1) are also responsible for nearly shore-parallel, eastward-directed, aeolian sand transport (Anthony, Vanhée, and Ruz, 2006). Based on wave and current measurements carried out in the intertidal and nearshore zones between Dunkirk and the Belgium border, Héquette *et al.* (2009) and Maspataud, Héquette, and Ruz, (2013) suggested that the nearshore bank and associated shore-parallel channel extending along the coast seaward of the *Dune Dewulf* and the *Dune Marchand* (Figure 2A) represent a barrier limiting onshore, wave-driven, sediment transport, and favoring

alongshore transport. In contrast, the low gradient nearshore slope offshore of the *Dune du Perroquet* (Figure 2A) would be more favorable to onshore-directed sand transport by wave oscillatory flows as shown in several studies carried out on gently sloping dissipative shorefaces (Aagaard *et al.*, 2004; Cooper and Navas, 2004). The increase in sediment supply to the east, either from longshore or nearshore sources, can likely explain the greater width of the upper beach along the *Dune du Perroquet* (Figure 10B) where the lowest storm impacts and the most significant dune development were observed (Figures 10C and 11).

As shown in a number of studies, the width of the upper beach is highly influential in determining the susceptibility of coastal dunes to erosion or to accretion, coastal dunes fringing a narrow upper beach being more vulnerable to erosion while dunes associated with a wide upper beach would be more stable or could develop upward and/or seaward (Crapoulet *et al.*, 2017; Hesp and Smyth, 2016; Houser, 2009; Keijsers *et al.*, 2014; Puijenbroek *et al.*, 2017; Pye and Blott, 2016a; Richter, Faust, and Maas, 2013; Saye *et al.*, 2005). Not only is a wide beach effective in dissipating wave energy, but a wider dry beach provides more sediment for aeolian transport to the adjoining coastal dunes. Moreover, a wide upper beach allows the seaward development of coastal dunes through the formation of incipient foredunes that can develop into a new established foredune. Even when incipient foredunes are ephemeral features that are eroded during subsequent storms associated with high water levels, they nevertheless protect the established foredune from erosion and hence contribute to shoreline stability. Dune height also shows some correspondence with dune front volume change, the lower dunes to the east tending to experience greater sediment accumulation compared to the higher dunes located westward (Figure 11). A similar relationship was found for the coastal dunes of microtidal barrier islands of the Gulf of Mexico by Houser *et al.* (2015) who observed that the rate of post-storm dune

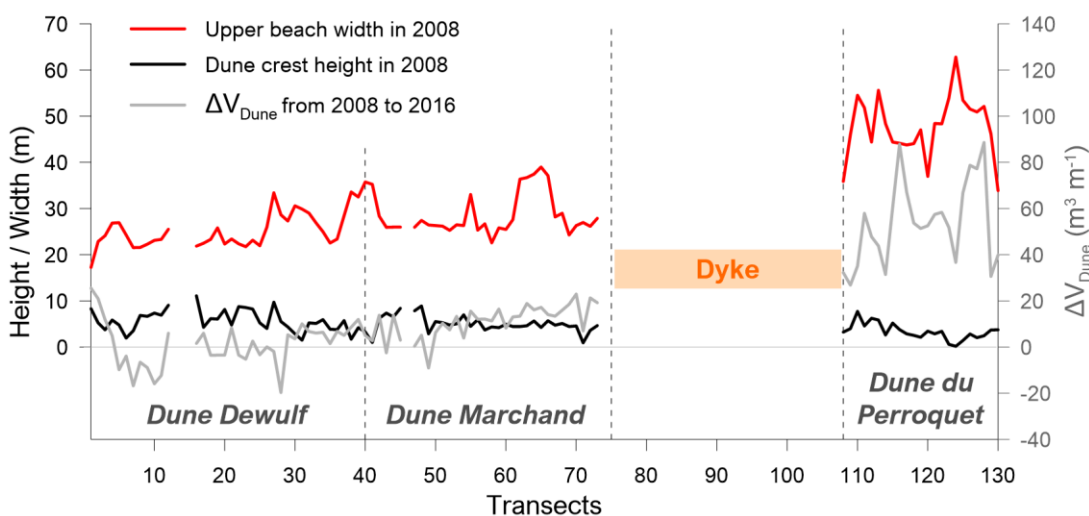


Figure 11. Longshore variations in upper beach width and dune crest height in 2008 and changes in dune volume from May 2008 to May 2016 based on airborne LiDAR topographic data (see Figure 10 for transects location).

recovery varied as a function of the initial dune height, the rate of recovery being fastest where the pre-storm dune heights were lower and slowest where the pre-storm heights were higher. However, along the macrotidal coast of northern France, dune height represents probably only a secondary parameter since large differences in dune volume change and in the rate of post-storm recovery are observed for similar dune heights in the western and central sectors of the study area (*i.e.*, *Dune Dewulf* and *Dune Marchand*) (Figures 10D and 11), whereas the initial upper beach width shows a much clearer relationship with dune volume change all along the coast (Figure 11).

Our results also show that coastal dunes were affected by episodic storm events that were responsible for significant changes taking place over short periods of time which were followed by much longer periods of recovery, similarly to what was observed in a number of previous studies (Castelle *et al.*, 2017; Houser *et al.*, 2015; Morton, Paine, and Gibeaut., 1994; Suanez *et al.*, 2015). From the mid-1990s to mid-2000s, the foredunes extending from Dunkirk to Bray Dunes (*Dune Dewulf* and *Dune Marchand*) (Figure 2) were in a state of mesoscale stability, with mild dune scarping in winter being generally followed by sand accumulation at the dune toe in spring and summer (Ruz, Anthony, and Faucon, 2005). In late March 2007, the storm No Name 1 of exceptionally long duration (Table 1) led to severe erosion along the foredune of the *Dune Dewulf* (Figure 7B) and to a lesser extent along the *Dune Marchand* (Figure 10D). This storm seems to have triggered major morphological changes in the foredune of the *Dune Dewulf* (Figure 7D) in response to the subsequent storms that occurred in late 2007 and early 2008 (Figure 5C). Our measurements show that the foredune in the westernmost sector underwent phases of partial dune recovery, whereas the upper beach could rapidly gain substantial volumes of sediment and fully recover within a time frame of a few weeks (Figure 7E), similarly to what was observed on other beaches (*e.g.*, Angnuureng *et al.*, 2017; Roberts, Wang, and Puleo, 2013). Full foredune recovery occurred over a much longer period of several years at the *Dune Dewulf* site (Figure 7D). After the scarping of the foredune front during the storms of 2007 and 2008, the stoss slope was very steep (Figure 7 C1), limiting aeolian accumulation on the dune crest. Subsequently, a significant amount of sand accumulated at the dune toe which formed a sand ramp (Figure 7 C2). This accumulation was then progressively stabilized by pioneer vegetation (*Elymus farctus*) and by marram grass (Figure 7 C3). The important role of dune ramps in beach/dune interactions has been acknowledged in several studies (Christiansen and Davidson-Arnott, 2004; Walker *et al.*, 2017), the presence of a sand ramp at the base of the dune being essential to provide a path for sand transport onto the stoss slope and towards the crest of the foredune. Once significant accumulation occurs at the dune toe, forming the ramp connecting the upper beach to the dune crest (Figure 7B), sand is then actively transferred landward along this gently-sloping surface and trapped by vegetation. The foredune recovery was initially slow after the storms of early 2008 and proceeded at a higher rate in 2012 and 2013. As underlined by Houser *et al.* (2015), the rate of dune recovery is initially small during the first few years after a storm, as long as vegetation does not colonize the dune front and traps wind-blown sand. The full recovery of the foredune at the *Dune Dewulf* site was furthermore favored by relatively calm

conditions between early 2009 and mid-2013, similarly to what was documented along the North Norfolk coastline, on the North Sea coast of England, where spatially differentiated alongshore recovery was observed during the same period (Brooks, Spencer, and Christie, 2017).

Following this phase of dune recovery, the coastline was hit by the series of storms of fall-winter 2013-2014 that were the most extreme sequence for 60 years that affected the west coast of Europe and southern North Sea (Brooks, Spencer, and Christie, 2017; Castelle *et al.*, 2015, 2017; Masselink *et al.*, 2016; Pye and Blott, 2016a; Suanez *et al.*, 2015; Wadey *et al.*, 2015). This storm cluster resulted in widespread erosion with dune scarping at the *Dune du Perroquet* (Figure 8B) and major dune front retreat and massive volume loss at the *Dune Dewulf* (Figure 7B,D). Dune erosion was much less significant in response to storms No Name 1 and Tilo in 2007 (Figure 7D) although wave energy during these events was considerably greater (Figure 5C). According to several studies, storm clustering can enhance coastal erosion, the impact of a single storm during a series of storms occurring at close intervals being influenced by the previous morphological state of the beach and dune (Dissanayake *et al.*, 2015; Karunaratna *et al.*, 2014; Splinter *et al.*, 2014). Because the beach level, and potentially the dune toe, is lowered during the first storms, increasing exposing the dune to wave attack, dune erosion may be larger during subsequent storms even of lower magnitude. It is possible that the succession of fall-winter 2013-2014 storms had large cumulative effects and increased foredune erosion at the *Dune Dewulf*. However, it is likely that the extreme water level (> 100-year return period) reached during storm Xaver on 6 December 2013 was the main cause of the severe erosion measured in early January 2014 (Figure 7 B,D), this storm surge having also been responsible for large impacts on other coastlines of the southwest North Sea (*e.g.*, Spencer *et al.*, 2015). The major role played by this extreme water level on dune erosion is confirmed at the *Dune du Perroquet* site where dune erosion in the fall-winter 2013-2014 was only observed immediately after storm Xaver and not after the preceding storms (Figure 8D). The beach/dune profiles surveyed after storms No Name 5 and Godehard revealed, on the contrary, that sand accumulated in the foredune (Figure 8D). The deposition of wind-blown sand in the foredune at this site was favored by the upper beach and dune front morphology, the width of the upper beach and the high elevation of the dune toe (Figures 10 A,B) preventing the dune front to be reached by waves, and the gentle slope of the stoss side of the foredune (Figure 8B) facilitating landward aeolian sand transfer from the upper beach to the dune. These results echo those obtained along the Narrabeen-Collaroy beach in southeast Australia by Splinter *et al.* (2018) who found that the elevation of the dune toe relative to storm water levels is a key factor explaining the alongshore variability in storm-induced dune erosion. Our surveys of upper beach/foredune evolution from 2007 to 2016 showed that the most energetic storm events, which occurred in 2007 and 2008 (Figure 5C), did not have the greatest impacts in terms of dune erosion (Figures 7D,8D). The storm event that particularly stands out from the 2007-2016 period is storm Xaver (5-6 December 2013) during which a spring tide combined with a 1.26 m surge at high tide resulted in an exceptionally high water level responsible for dramatic erosion. Along macrotidal coasts, the impacts of storms on dune erosion

is particularly dependent on the concomitance of storm surge and high-energy waves with the timing of high tides (Esteves *et al.*, 2012; Masselink *et al.*, 2016; Pye and Blott, 2008; Ruz and Meur-Férec, 2004; Ruz, Héquette, and Maspataud, 2009). From our analyses of storm impacts since 2007, it appears that wave energy at high tide is not necessarily the major parameter controlling coastal dune erosion, but the height of water level reached during the storm that allows, or not, the dune toe to be reached by waves. In addition, for a same offshore wave energy level, wave impacts on the dune front are probably enhanced during very high water levels due to reduced wave dissipation across the upper beach.

With rising sea-level due to climate change, (IPCC, 2013), storm water levels will progressively reach higher elevations and high critical water levels responsible for dune erosion will be reached more frequently. In a study based on tide gauge data collected on the British coast of the English Channel and considering a moderate rise in sea-level of 40 cm by 2100, Haigh, Nicholls, and Wells (2011) estimated that, the return period of high water levels that had a 100-year return period in 1990 will be 1 year on average by the end of the 21<sup>st</sup> century. Because a minimum time period is required for a coastal dune to recover after storm erosion, and since the return periods of extreme water levels will shorten in the future, coastal dunes may not have sufficient time to fully recover between storms and may become increasingly vulnerable to wave erosion, which may result in higher dune front erosion, especially where sediment supply is limited. This is notably the case in the western sector of the study area (*Dune Dewulf*) where the coastal dune is already highly vulnerable to high water levels (Figure 7) and characterized by low to moderate sediment accumulation rates (Figure 10D). Conversely, where sediment supply is high and the coastal dunes experience high sediment accumulation rates, such as in the *Dune du Perroquet* sector (Figures 8 and 10D), dunes may continue to develop and prograde seaward even under rising sea-level. Extensive seaward shoreline displacement associated with foredune development occurred throughout the 20<sup>th</sup> century near Calais (Ruz *et al.*, 2017), for example, while sea-level was rising, due to large sediment supply from the shoreface (Héquette and Aernouts, 2010). However, because the frequency of high water levels will increase in the future with sea-level rise, it is not known if incipient foredunes will be able to continue to develop and extend seaward.

### CONCLUSIONS

The impacts of storms on the upper beach and coastal dunes extending between Dunkirk and the Belgium border, northern coast of France, and their post-storm recovery were analyzed using nearly 10 years of offshore wave measurements, water level records, and beach and foredune topographic surveys. Our results indicate a strong alongshore variability in dune erosion and recovery with a positive eastward gradient in dune volume change related to longshore and onshore-directed sediment supply. The westernmost foredunes are more prone to erosion, which can be explained by lower elevations of the upper beach/dune toe contact and narrower upper beach widths compared to the eastern sector where the foredune shows a much lower susceptibility to erosion.

Our measurements revealed that even where the foredune underwent significant erosion during the first years of the survey period, progressive full dune recovery took place through the

development of a sand ramp at the dune toe that favored landward sediment transport from the upper beach to the stoss slope of the foredune, which was favored by relatively calm conditions during several years. This period was followed by an unusual series of closely spaced storms during fall-winter 2013-2014 that had major impacts on the coasts of Western Europe. These storms were not associated with particularly high energy waves, but they have been responsible for extreme water levels largely above HAT, especially during storm Xaver in early December 2013 when the 100-year return period water level was exceeded, which resulted in widespread erosion and significant retreat of the dune front in the western sector accompanied by massive volume loss. Because sea-level rise is expected to accelerate in the future due to climate change, storm water levels will progressively reach higher elevations and the return periods of extreme water levels responsible for coastal dune erosion will shorten, which will likely result in less dune recovery and therefore in more significant dune erosion. However, because our results showed significant alongshore variability in coastal dune response to storm events and in post-storm recovery over short distances, future shoreline change will likely also be variable, depending on local sediment supply and upper beach morphology. In order to provide reliable estimates of coastal dune evolution in the next decades, which is of critical importance for coastal management, it is essential to continue conducting detailed beach/dune monitoring in the future.

### ACKNOWLEDGEMENTS

This study was partly funded by French *Centre National de la Recherche Scientifique* (CNRS) and the French Department of Higher Education and Research through operating research funds to the Laboratoire d'Océanologie et de Géosciences. Wind data were obtained by courtesy of *Météo-France* through a research agreement with the *Université du Littoral Côte d'Opale*. Water level and bathymetry data were obtained from the French Hydrographic Survey (SHOM). Offshore wave data were kindly provided by the Flanders Marine Institute (VLIZ). The 2008 LiDAR data were obtained from the DDTM of the *Département du Nord*, the subsequent LiDAR data were obtained through the interregional program CLAREC funded by the Regional Councils of Normandy, Picardie and Nord-Pas de Calais and by the French CNRS, except for the 2016 LiDAR data that were collected by the CIRCLE of the University of Caen thanks to funding from the SNO DYNALIT. We gratefully acknowledge the constructive comments from two anonymous reviewers and from Bruno Castelle, Associate Editor of this Special Issue.

### LITERATURE CITED

- Aagaard, T.; Davidson-Arnott, R.; Greenwood, B., and Nielsen, J., 2004. Sediment supply from shoreface to dunes: linking sediment transport measurements and long-term morphological evolution. *Geomorphology*, 60(1-2), 204-224.
- Aernouts, D. and Héquette, A., 2006. Coastline and shoreface evolution in the Bay of Wissant, Pas-de-Calais, France. *Géomorphologie : relief, processus, environnement*, 12(1), 49-64.
- Angnuureng, D. B.; Almar, R.; Senechal, N.; Castelle, B.; Addo K.A.; Marieu, V., and Ranasinghe R., 2017. Shoreline

- resilience to individual storms and storm clusters on a meso-macrotidal barred beach. *Geomorphology*, 290, 265-276.
- Anthony, E.J., 2013. Storms, shoreface morphodynamics, sand supply, and the accretion and erosion of coastal dune barriers in the southern North Sea. *Geomorphology*, 199, 8-21.
- Anthony, E.J.; Levoy, F.; Montfort, O., and Degryse-Kulkarni, C., 2005. Patterns of short-term intertidal bar mobility on a ridge and runnel beach, Merlimont, Northern of France. *Earth Surface Processes and Landforms*; 30(1), 81-93.
- Anthony, E.J.; Ruz, M.H., and Vanhée, S., 2009. Aeolian sand transport over complex intertidal bar-trough beach topography. *Geomorphology*, 105(1-2), 95-105.
- Anthony, E.J.; Vanhée, S., and Ruz, M.H., 2006. Short-term beach-dune sand budgets on the North Sea coast of France: sand supply from shoreface to dunes and the role of wind and fetch. *Geomorphology*, 81(3-4), 316-329.
- Augris, C.; Clabaut, P., and Vicaire, O., 1990. *Le domaine marin du Nord-Pas-de-Calais – Nature, morphologie et mobilité des fonds*. Edition IFREMER – Région Nord-Pas-de-Calais, 93 p.
- Bagnold, R.A., 1941. *The physics of wind blown sands and desert dunes*. London, Methuen, 265 p.
- Battiau-Queney, Y.; Billet, J.F.; Chaverot, S. and Lanoy-Ratel, P., 2003. Recent shoreline mobility and geomorphologic evolution of macrotidal sandy beaches in the north of France. *Marine Geology*, 194(1-2), 31-45.
- Battiau-Queney, Y.; Fauchois, J.; Deboudt, P., and Lanoy-Ratel, P., 2001. Beach-dune systems in a macrotidal environment along the northern French coast. *Journal of Coastal Research*, Special Issue No 34, pp. 580-592.
- Bauer, B.O. and Davidson-Arnott, R.G.D., 2003. A general framework for modeling sediment supply to coastal dunes including wind angle, beach geometry, and fetch effects. *Geomorphology*, 49(1-2), 89-108.
- Bauer, B.O.; Davidson-Arnott, R.G.D., and Hesp, P.A., Namikas, S.L., Ollerhead, J., and Walker, I.J., 2009. Aeolian sediment transport on a beach: Surface moisture, wind fetch, and mean transport. *Geomorphology*, 105(1-2), 106-116.
- Beck, C.; Clabaut, P.; Dewez, S.; Vicaire, O.; Chamley, H.; Augris, C.; Hoslin, R., and Caillot, A., 1991. Sand bodies and sand transport paths at the English Channel-North Sea border: morphology, dynamics and radioactive tracing. *Oceanologica Acta*, 11, 111-121.
- Brooks, S.M.; Spencer, T., and Christie, E.K., 2017. Storm impacts and shoreline recovery: Mechanisms and controls in the southern North Sea. *Geomorphology*, 283, 48-60.
- Burvingt, O.; Masselink, G.; Russell, P., and Scott, T., 2017. Classification of beach response to extreme storms. *Geomorphology*, 295, 722-737.
- Burvingt, O.; Masselink, G.; Scott, T.; Davidson, M., and Russell, P., 2018. Climate forcing of regionally-coherent extreme storm impact and recovery on embayed beaches. *Marine Geology*, 401, 112-128.
- Cartier, A. and Héquette, A., 2011. Variation in longshore sediment transport under low to moderate energy conditions on barred macrotidal beaches. *Journal of Coastal Research*, Special Issue No 64, pp. 45-49.
- Cartier, A. and Héquette, A., 2013. The influence of intertidal bar-trough morphology on sediment transport on macrotidal beaches, Northern France. *Zeitschrift für Geomorphologie*, 57(3), 325-347.
- Castelle, B.; Bujan, S.; Ferreira, S., and Dodet, G., 2017. Foredune morphological changes and beach recovery from the extreme 2013/2014 winter at a high-energy sandy coast. *Marine Geology*, 385, 41-55.
- Castelle, B.; Marieu, V.; Bujan, S.; Splinter, K.D.; Robinet, A.; Sénéchal, N., and Ferreira, S., 2015. Impact of the winter 2013-2014 series of severe Western Europe storms on a double-barred sandy coast: Beach and dune erosion and megacusp embayments. *Geomorphology*, 238, 135-148.
- Chaverot, S.; Héquette, A., and Cohen, O., 2008. Changes in storminess and shoreline evolution along the northern coast of France during the second half of the 20th century. *Zeitschrift für Geomorphologie*, Supp. Bd. 52(3), 1-20.
- Christiansen, M.B. and Davidson-Arnott, R.G.D., 2004. Rates of landward sand transport over the foredune at Skallingen, Denmark and the role of dune ramps. *Geografisk Tidsskrift*, 104(1), 31-43.
- Clabaut, P.; Chamley, H., and Marteel, H., 2000. Evolution récente des dunes littorales à l'est de Dunkerque (Nord de la France). *Géomorphologie : relief, processus, environnement*, 6(2), 125-136.
- Cooper, J.A.G.; Jackson, D.W.T.; Navas, F.; McKenna, J., and Malvarez, G., 2004. Identifying storm impacts on an embayed, high-energy coastline: examples from western Ireland. *Marine Geology*, 210, 261-280.
- Cooper, J.A.G. and Navas, F., 2004. Natural bathymetric change as a control on century-scale shoreline behavior. *Geology*, 32(6), 513-516.
- Crapoulet, A., Héquette, A., Bretel, P., and Levoy, F., 2014. Détermination de la position du trait de côte à partir de levés topographiques LiDAR aéroportés. *XIII<sup>èmes</sup> Journées Nationales de Génie Côtier – Génie Civil*, Dunkirk, 2-4 July 2014, pp. 565-572.
- Crapoulet, A.; Héquette, A.; Marin, D.; Levoy, F., and Bretel, P., 2017. Variations in the response of the dune coast of Northern France to major storms as a function of available beach sediment volume. *Earth Surface Processes and Landforms*, 42(11), 1603-1622.
- Daubord, C., 2014. *Caractérisation de 7 évènements de tempête de l'automne-hiver 2013-2014 à partir des données disponibles au SHOM*. Brest, Technical report of the Service Hydrographique et Océanographique de la Marine N° 001/2014, 37 p.
- Davidson-Arnott, R.G.D. and Bauer, B.O., 2009. Aeolian sediment transport on a beach: Thresholds, intermittency, and high frequency variability. *Geomorphology*, 105(1-2), 117-126.
- Davidson-Arnott, R.G.D.; MacQuarrie, K., and Aagaard, T., 2005. The effect of wind gusts, moisture content and fetch length on sand transport on a beach. *Geomorphology*, 68(1-2), 115-129.
- Davidson-Arnott, R.G.D. and Stewart, C.J., 1987. The effect of longshore sand waves on dune erosion and accretion, Long Point, Ontario. In: *Proceedings of the Canadian Coastal Conference*, Quebec, pp. 131-144.
- de Winter, R.C.; Gongriep, F., and Ruessink, B.G., 2015. Observations and modeling of alongshore variability in dune

- erosion at Egmond aan Zee, the Netherlands. *Coastal Engineering*, 99, 167-175.
- Dissanayake, P.; Brown, J.; Wisse, P., and Karunarathna, H., 2015. Effects of storm clustering on beach/dune evolution. *Marine Geology*, 370, 63-75.
- Dong, Z.; Liu, X.; Wang, H., and Wang, X., 2003. Aeolian sand transport: A wind tunnel model. *Sedimentary Geology*, 161(1-2), 71-83.
- Doyle, T.B. and Woodroffe, C.D., 2018. The application of LiDAR to investigate foredune morphology and vegetation. *Geomorphology*, 303, 106-121.
- Esteves, L.S.; Brown, J.M.; Williams, J.J., and Lymbery, G., 2012. Quantifying thresholds for significant dune erosion along the Sefton Coast, Northwest England. *Geomorphology*, 143-144, 52-61.
- Haigh, I.; Nicholls, R., and Wells, N., 2011. Rising sea levels in the English Channel 1900 to 2100. *Proceedings of ICE-Maritime Engineering*, 164(2), 81-92.
- Hanley, M.E.; Hoggart, S.P.G.; Simmonds, D.J.; Bichot, A.; Colangelo, M.A.; Bozzeda, F.; Heurtefeux, H.; Ondiviela, B.; Ostrowski, R.; Recio, M.; Trude, R.; Zawadzka-Kahlau, E., and Thompson, R.C., 2014. Shifting sands? Coastal protection by sand banks, beaches and dunes. *Coastal Engineering*, 87, 136-146.
- Harley, M.D.; Turner, I.L.; Short, A.D., and Ranasinghe, R., 2009. An empirical model of beach response to storms – SE Australia. In Proceedings “Coasts and Ports 2009: In a Dynamic Environment”, Wellington, New Zealand, pp. 600-606.
- Héquette, A. and Aernouts, D., 2010. The influence of nearshore sand bank dynamics on shoreline evolution in a macrotidal coastal environment, Calais, Northern France. *Continental Shelf Research*, 30(12), 1349-1361.
- Héquette, A. and Cartier, A., 2016. Theoretical and observed breaking wave height on a barred macrotidal beach: implications for the estimation of breaker index on beaches with large tidal range. *Journal of Coastal Research*, Special Issue No 75, pp. 861-866.
- Héquette, A.; Hemdane, Y., and Anthony, E.J., 2008a. Sediment transport under wave and current combined flows on a tide-dominated shoreface, northern coast of France. *Marine Geology*, 249(3-4), 226-242.
- Héquette, A.; Hemdane, Y., and Anthony, E.J., 2008b. Determination of sediment transport paths in macrotidal shoreface environments: a comparison of grain-size trend analysis with near-bed current measurements. *Journal of Coastal Research*, 24(3), 695-707.
- Héquette, A.; Ruz, M.H.; Maspataud, A., and Sipka, V., 2009. Effects of nearshore sand bank and associated channel on beach hydrodynamics : implications for beach and shoreline evolution. *Journal of Coastal Research*, Special Issue No 56, pp. 59-63.
- Hesp, P.A., 1988. Surfzone, beach and foredune interactions on the Australian south east coast. *Journal of Coastal Research*, Special Issue No 3, 15-25.
- Hesp, P.A., 2002. Foredunes and blowouts: initiation, geomorphology and dynamics. *Geomorphology*, 48, 245-268.
- Hesp, P.A., 2011. Dune coasts. In: E. Wolanski and D.S. McLusky (eds.), *Treatise on Estuarine and Coastal Science*, 3, pp. 193-221.
- Hesp, P.A. and Smyth T.A.G., 2016. Surfzone-beach-dune interactions: Flow and sediment transport across the intertidal beach and backshore. *Journal of Coastal Research*, Special Issue No 75, pp. 8-12.
- Hesp, P.A. and Walker, I.J., 2013. Aeolian environments: coastal dunes. In: Shroder, J., Lancaster, N., Sherman, D.J., Baas, A.C.W. (Eds.), *Treatise on Geomorphology*, Vol. 11, Aeolian Geomorphology, Academic Press, San Diego, pp. 109-133.
- Houser, C., 2009. Synchronization of transport and supply in beach-dune interaction. *Progress in Physical Geography*, 33(6), 733-746.
- Houser, C., 2013. Alongshore variation in the morphology of coastal dunes: Implications for storm response. *Geomorphology*, 199, 48-61.
- Houser, C. and Ellis, J., 2013. Beach and dune interaction. In: Shroder, J. (Editor in Chief), Sherman, D.J. (Ed.), *Treatise on Geomorphology*, Vol. 10, Coastal Geomorphology, Academic Press, San Diego, pp. 267-288.
- Houser, C. and Hamilton, S., 2009. Sensitivity of post-hurricane beach and dune recovery to event frequency. *Earth Surface Processes and Landforms*, 34(5), 613-628.
- Houser, C.; Hapke, C., and Hamilton, S., 2008. Controls on coastal dune morphology, shoreline erosion and barrier island response to extreme storms. *Geomorphology*, 100(3-4), 223-240.
- Houser, C.; Wernette, P.; Rentschlar, E.; Jones, H.; Hammond, B., and Trimble, S., 2015. Post-storm beach and dune recovery: Implications for barrier island resilience. *Geomorphology*, 234, 54-63.
- Idier, D.; Balouin, Y.; Bohn Bertoldo, R.; Bouchette, F.; Boulahya, F.; Brivois, O.; Calvete, D.; Capo, S.; Castelle, B.; Certain, R.; Charles, E.; Chateauminois, E.; Delvallée, E.; Falqués, A.; Fattal, P.; Larroudé, P.; Lecacheux, S.; Garnier, R.; Héquette, A.; Le Cozannet, G.; Maanan, M.; Mallet, C.; Maspataud, A.; Oliveros, C.; Paillart, M.; Parisot, J.P.; Pedreros, R.; Poumadère, M.; Robin, N.; Ruz, M.H.; Robin, M.; Thiébot, J., and Vinchon, C., 2013. Vulnerability of sandy coasts to climate variability. *Climate Research*, 57, 19-44.
- IPCC, 2013. *Climate change 2013: The Physical Science Basis*. Contribution of Working Group I to the Fifth Assessment Report of the Intergovernmental Panel on Climate Change , T.F. Stocker *et al.* (eds.), Cambridge University Press, Cambridge, 1535 p.
- Kahn, J.H. and Roberts, H., 1982. Variations in storm response along a microtidal transgressive barrier-island arc. *Sedimentary Geology*, 33(2), 129-146.
- Karunarathna, H.; Pender, D.; Ranasinghe, R.; Short, A.D., and Reeve, D.E., 2014. The effects of storm clustering on beach profile variability. *Marine Geology*, 348, 103-112.
- Katuna, M.P., 1991. The effects of Hurricane Hugo on the Isle of Palms, South Carolina: from destruction to recovery. *Journal of Coastal Research*, Special Issue No 8, pp. 263-273.
- Keijsers, J.G.S.; Poortinga, A.; Riksen, M.J.P.M., and Maroulis, J., 2014. Spatio-temporal variability in accretion and erosion

- of coastal foredunes in the Netherlands: Regional climate and local topography. *PLoS ONE* 9: e91115.
- Larson, M.; Erikson, L., and Hanson, H., 2004. An analytical model to predict dune erosion due to wave impact. *Coastal Engineering*, 51, 675-696.
- Le Mauff, B.; Juigner, M.; Ba, A.; Robin, M.; Launeau, P., and Fattal, P., 2018. Coastal monitoring solutions of the geomorphological response of beach-dune systems using multi-temporal LiDAR datasets (Vendée coast, France). *Geomorphology*, 304, 121-140.
- Levoy, F.; Anthony, E.J.; Monfort, O.; Robin, N., and Bretel, P., 2013. Formation and migration of transverse bars along a tidal sandy coast deduced from multi-temporal Lidar datasets. *Marine Geology*, 342, 39-52.
- Lettau, K. and Lettau, H., 1977. Experimental and micrometeorological field studies of dune migration. In: H. Lettau and K. Lettau (eds.), *Exploring the World's Driest Climate*, IES Report, vol. 101, University of Wisconsin Press, Madison, pp. 110-147
- Loureiro, C.; Ferreira, O., and Cooper, J.A.G., 2012. Extreme erosion on high-energy embayed beaches: influence of megarips and storm grouping. *Geomorphology*, 139-140, 155-171.
- Maspataud, A.; Ruz, M.H., and Héquette, A., 2009. Spatial variability in post-storm beach recovery along a macrotidal barred beach, southern North Sea. *Journal of Coastal Research*, Special Issue No 56, pp. 88-92.
- Maspataud, A.; Ruz, M.H., and Héquette, A., 2011. Storm-driven shoreline evolution on a macrotidal coast : short- to medium-term spatial variability. A case study on the northern coast of France. *Proceedings Coastal Sediments '11*, 7<sup>th</sup> Int. Symp. Coastal Eng. Miami, USA, 2-6 May 2011, pp. 927-940.
- Maspataud, A.; Héquette, A., and Ruz, M.H., 2013. Contrasting hydrodynamic and morphologic response to fair-weather and storm conditions along southern North Sea coast (East of Dunkirk, France). *Proceedings Coastal Dynamics 2013*, Bordeaux, 24-28 June 2013, pp. 1147-1158.
- Maspataud, A.; Ruz, M.H., and Vanhée, S., 2012. Potential impacts of extreme storm surges on a low-lying densely populated coastline: the case of Dunkirk area, Northern France. *Natural Hazards*, 66(3), 1327-1343.
- Masselink, G.; Austin, M.; Scott, T.; Poate, T., and Russel, P., 2014. Role of wave forcing, storms and NAO in outer bar dynamics on a high-energy, macro-tidal beach. *Geomorphology*, 226, 76-93.
- Masselink, G.; Scott, T.; Poate, T.; Russell, P.; Davidson, M., and Conley, D., 2016. The extreme 2013/2014 winter storms: hydrodynamic forcing and coastal response along the southwest coast of England. *Earth Surface Processes and Landforms*, 41(3), 378-391.
- Mathew, S.; Davidson-Arnott, R.G.D., and Ollerhead, J., 2010. Evolution of beach/dune system following overwash during catastrophic storm: Greenwich dunes, Prince Edward Island 1936-2005. *Canadian Journal of Earth Sciences*, 47, 273-290.
- Matthews, T.; Murphy, C.; Wilby, R.L., and Harrigan, S., 2014. Stormiest winter on record for Ireland and the UK. *Nature Climate Change*, 4(9), 738-740.
- Morton, R.A.; Paine, J.G., and Gibeaut, J.C., 1994. Stages and duration of post-storm beach recovery, southeastern Texas coast, U.S.A. *Journal of Coastal Research*, 10(4), 884-908.
- Neumann, B.; Vafeidis, A.T., Zimmermann, J., and Nicholls, R.J., 2015. Future coastal population growth and exposure to sea-level rise and coastal flooding - A global assessment. *PLoS One*, 10(3): e0118571.
- Nicholls, R.J. and Cazenave, A., 2010. Sea-level rise and its impact on coastal zones. *Science*, 328 (5985), 1517-1520.
- Pinna, M.S.; Canadas, E.M.; Fenu, G., and Bacchetta, G., 2015. The European *Juniperus* habitat in the Sardinian coastal dunes: Implication for conservation. *Estuarine, Coastal and Shelf Science*, 164, 214-220.
- Puijenbroek, M.E.B. van; Limpens, J.; de Groot, A.V.; Riksen, M.J.P.M.; Gleichman, M.; Slim, P.A.; Dobben, H.F. van, and Berendse, F. 2017. Embryo dune development drivers: beach morphology, growing season precipitation, and storms. *Earth Surface Processes and Landforms*, 42(11), 1733 – 1744.
- Psuty, N.P., 1988. Sediment budget and dune/beach interaction. *Journal of Coastal Research*, Special Issue No 3, pp. 1-4.
- Pye, K. and Blott, S.J., 2008. Decadal-scale variation in dune erosion and accretion rates: An investigation of the significance of changing storm tide frequency and magnitude on the Sefton coast, UK. *Geomorphology*, 102(3-4), 652-666.
- Pye, K. and Blott, S.J., 2016a. Assessment of beach and dune erosion and accretion using LiDAR: Impact of the stormy 2013-14 winter and longer term trends on the Sefton Coast, UK. *Geomorphology*, 266, 146-167.
- Pye, K. and Blott, S.J., 2016b. The relative effect of the UK's stormy winter 2013-2014 on dune erosion: Case study of the Sefton Coast, Northwest England. *Shore & Beach*, 84(2), 31-48.
- Pye, K., Saye, S. and Blott, S., 2007. *Sand dune processes and management for flood and coastal defence - Part 1: Project overview and Recommendations*. Department for Environment, Food and Rural, London (Great-Britain), Technical Report FD1302/TR, 63 pp.
- Reichmüth, B. and Anthony, E.J., 2007. Tidal influence on the intertidal bar morphology of two contrasting macrotidal beaches. *Geomorphology*, 90(1-2), 101 - 114.
- Richter, A.; Faust, D., and Maas, H.G., 2013. Dune cliff erosion and beach width change at the northern and southern spits of Sylt detected with multi-temporal Lidar. *Catena*, 103: 103-111.
- Roberts, T.M.; Wang, P., and Puleo, J.A., 2013. Storm-driven cyclic beach morphodynamics of a mixed sand and gravel beach along the Mid-Atlantic Coast, USA. *Marine Geology*, 346, 403-421.
- Rufin-Soler, C.; Héquette, A., and Gardel, A., 2008. Assessing the vulnerability of coastal lowlands to marine flooding using LIDAR data, Sangatte coastal dunes, northern France. *Zeitschrift für Geomorphologie*, Supp. Bd. 52(3), 195-211.
- Ruggiero, P.; Komar, P.D.; McDouglas, W.G.; Marra, J.J., and Beach, R.A., 2001. Wave runup, extreme water levels and erosion of properties backing beaches. *Journal of Coastal Research*, 17(2), 407-419.
- Ruz, M.H.; Anthony, E.J., and Faucon, L., 2005. Coastal dune evolution on a shoreline subject to strong human pressure:

- the Dunkirk area, northern France. In Proceedings 'Dunes and Estuaries 2005', International Conference on Nature Restoration Practices in European Coastal Habitats, Koksijde, Belgium, 19-23 September 2005, pp. 441-449.
- Ruz, M.H.; Héquette, A., and Marin, D., 2017. Development of large nebkhas along an accreting macrotidal coastline, Northern France. *Aeolian Research*, 24, 1-14.
- Ruz, M.-H.; Héquette, A.; Marin, D.; Sipka, V.; Crapoulet, A., and Cartier, A., 2017b. Development of an incipient foredune field along a prograding macrotidal shoreline, northern France. *Géomorphologie : relief, processus, environnement*, 23(1), 37-50.
- Ruz, M.H.; Héquette, A., and Maspataud, A., 2009. Identifying forcing conditions responsible for foredune erosion on the northern coast of France. *Journal of Coastal Research*, Special Issue No 56, pp. 356-360.
- Ruz, M.H. and Meur-Férec, C., 2004. Influence of high water levels on aeolian sand transport: upper-beach/dune evolution on a macrotidal coast, Wissant Bay, Northern France. *Geomorphology* 60(1-2), 73-87.
- Saye, S.; van der Wal, D.; Pye, K., and Blott, S., 2005. Beach-dune morphological relationships and erosion/accretion: An investigation at five sites in England and Wales using LIDAR data. *Geomorphology*, 72(1-4), 128-155.
- Scott, T.; Masselink, G.; O'Hare, T.; Saulter, A.; Poate, T.; Russell, P.; Davidson, M., and Conley, D. 2016. The extreme 2013/2014 winter storms: Beach recovery along the southwest coast of England. *Marine Geology*, 382, 224-241.
- Spalding, M.D.; Ruffo, S.; Lacambra, C.; Meliane, I.; Hale, L.Z.; Shepard, C.C., and Beck, M.W., 2014. The role of ecosystems in coastal protection: Adapting to climate change and coastal hazards. *Ocean & Coastal Management*, 90, 50-57.
- Spencer, T.; Brooks, S.M.; Evans, B.R.; Tempest, J.A., and Möller, I., 2015. Southern North Sea storm surge event of 5 December 2013: Water levels, waves and coastal impacts. *Earth-Science Reviews*, 146, 120-145.
- Splinter, K.D.; Carley, J.T.; Golshani, A., and Tomlinson, R., 2014. A relationship to describe the cumulative impact of storm clusters on beach erosion. *Coastal Engineering*, 83, 49-55.
- Splinter, K.D.; Kearney, E.T., and Turner, I.L., 2018. Drivers of alongshore variable dune erosion during a storm event: Observations and modelling. *Coastal Engineering*, 131, 31-41.
- Suanez, S.; Cancouët, R.; Floc'h, F.; Blaise, E.; Arduin, F.; Filipot, J.-F.; Cariolet, J.-M., and Delacourt, C., 2015. Observations and predictions of wave runup, extreme water levels, and medium-term dune erosion during storm conditions. *Journal of Marine Science and Engineering*, 3(3), 674-698.
- Suanez, S.; Cariolet, J.-M.; Cancouët, R.; Arduin, F., and Delacourt, C., 2012. Dune recovery after storm erosion on a high-energy beach: Vougot Beach, Brittany (France). *Geomorphology*, 139-140, 16-33.
- Van der Biest, K.; De Nocker, L.; Provoost, S.; Boerema, A.; Staes, J., and Meire, P., 2017. Dune dynamics safeguard ecosystem services. *Ocean & Coastal Management*, 149, 148-158.
- Vasseur, B. and Héquette, A., 2000. Storm surges and erosion of coastal dunes between 1957 and 1988 near Dunkerque (France), southwestern North Sea. In : K. Pye and J.R.L. Allen (eds.) : *Coastal and Estuarine Environments*, Geological Society, London, Special Publications, 175, pp. 99-107.
- Wadey, M.P.; Brown, J.M.; Haigh, I.D.; Dolphin, T., and Wisse, P., 2015. Assessment and comparison of extreme sea levels and waves during the 2013/14 storm season in two UK coastal regions. *Natural Hazards and Earth System Sciences*, 15, 2209-2225.
- Wahl, T.; Haigh, I.D.; Nicholls, R.J.; Arns, A.; Dangendorf, S.; Hinkel, J., and Slangen, A.B.A., 2017. Understanding extreme sea levels for broad-scale coastal impact and adaptation analysis. *Nature Communications*, 8, 16075. doi: 10.1038/ncomms16075.
- Walker, I.J.; Davidson-Arnott, R.G.D.; Bauer, B.O.; Hesp, P.A.; Delgado-Fernandez, I.; Ollerhead, J., and Smyth, T.A.G., 2017. Scale-dependent perspectives on the geomorphology and evolution of beach-dune systems. *Earth-Science Reviews*, 171, 220-253.
- Woolard, J.W. and Colby, J.D., 2002. Spatial characterization, resolution, and volumetric change of coastal dunes using airborne LIDAR: Cape Hatteras, North Carolina. *Geomorphology*, 48(1-3), 269-287.